Mitglied der Helmholtz-Gemeinschaft

Protein structures and equilibrium dynamics as seen by neutrons

FEBS Advanced Course 2022, **Biomolecules in Action III**
DESY, Hamburg

June 22nd 2022 | Tobias E. Schrader

Outline

- Motivation: Why do we need protein structures at atomic resolution measured with neutrons?
- neutron protein crystallography
- one application example: M^{pro} of SARS-CoV2
- Small angle neutron scattering
- Contrast matching with small angle neutron scattering
- one application example: matched bicelles for membrane proteins
- Neutron Spin Echo (NSE) Technique as one inelastic neutron scattering technique
- One application expample of NSE: Phosphoglyceratkinase (PGK)
- Summary

The protein/enzyme β-lactamase

β-lactamase: An enzyme that destroys β-lactam antibiotics

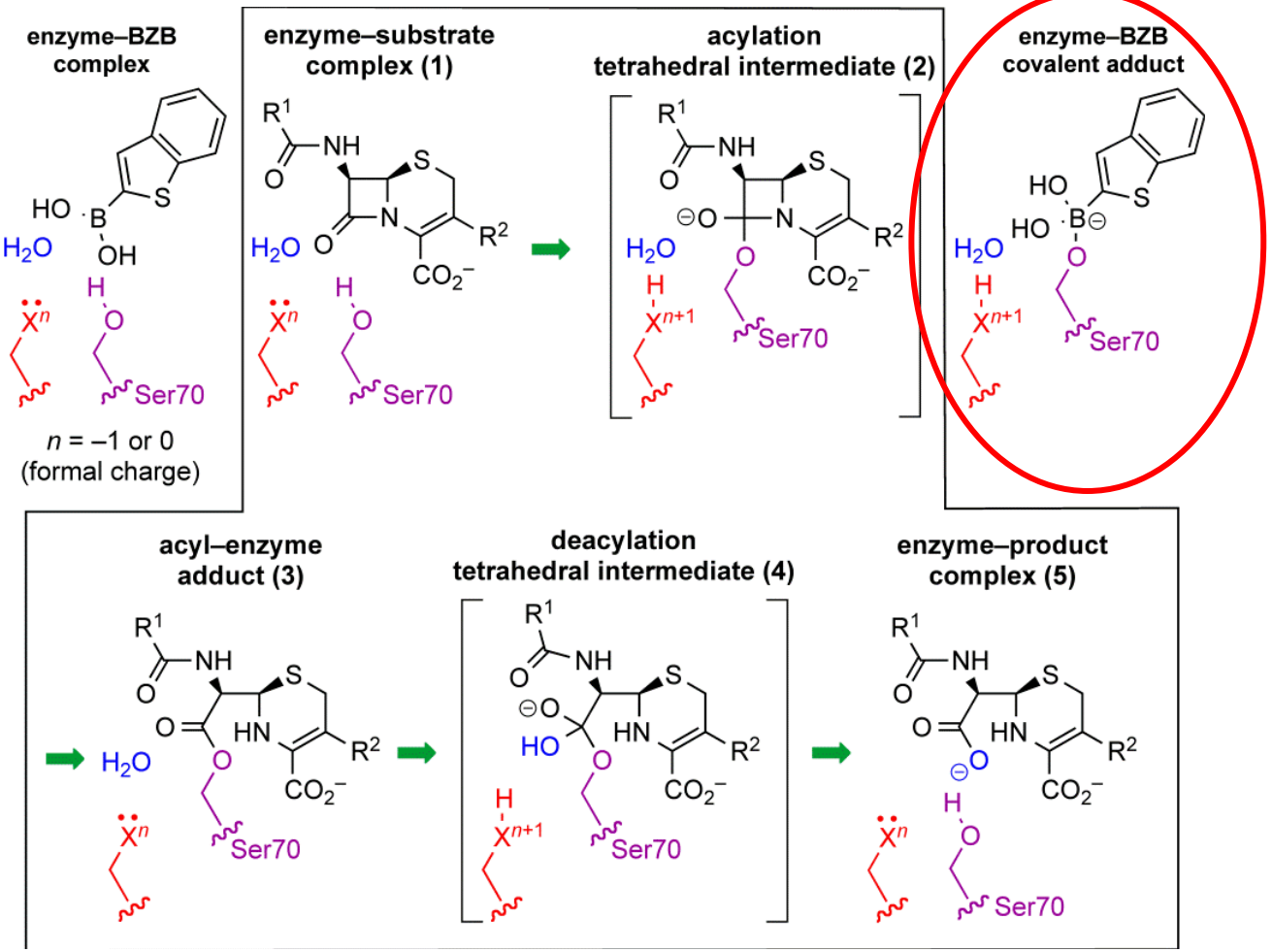

The catalytic cycle of a class A β-lactamase illustrated for a cephalosporin substrate (inside box) and the mode of inhibition by BZB (outside box). The general base employed is not necessarily the same for acylation and deacylation. The overall reaction pathway for β-lactam hydrolysis of a cephalosporin-like substrate by the class A β-lactamase enzymes.

Figures from: Tomanicek et al., doi: 10.1074/jbc.M112.436238

Catalytic Proton Network of the Toho-1 β-Lactamase

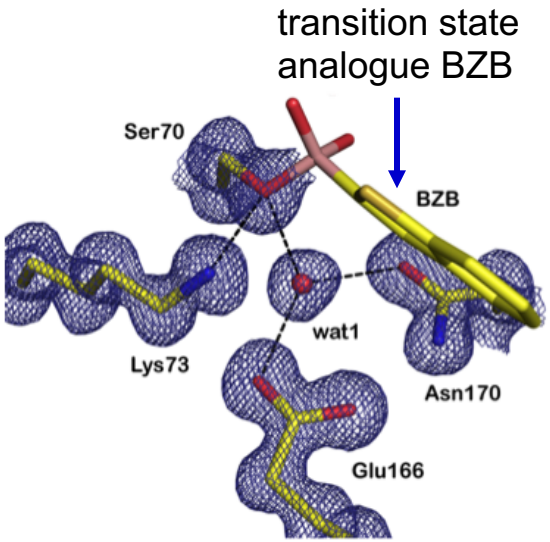

electron density map

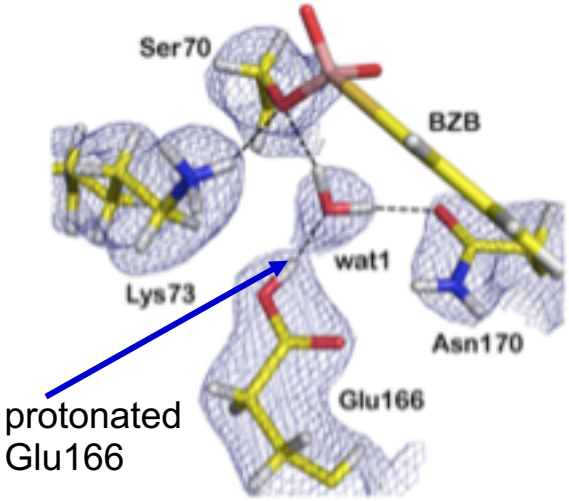

nuclear density map from BioDiff

Glu166 acts as the general base during the catalytic action of the enzyme.

Stephen J. Tomanicek, Robert F. Standaert, Kevin L. Weiss,
Andreas Ostermann, Tobias E. Schrader, Joseph D. Ng, and Leighton Coates
J. Biol. Chem. 2013, 288:4715-4722

Most structures are obtained by x-ray crystallography, available neutron structures in protein data bank: ca. 200

Entries in the protein data base as of 9th of May 2022

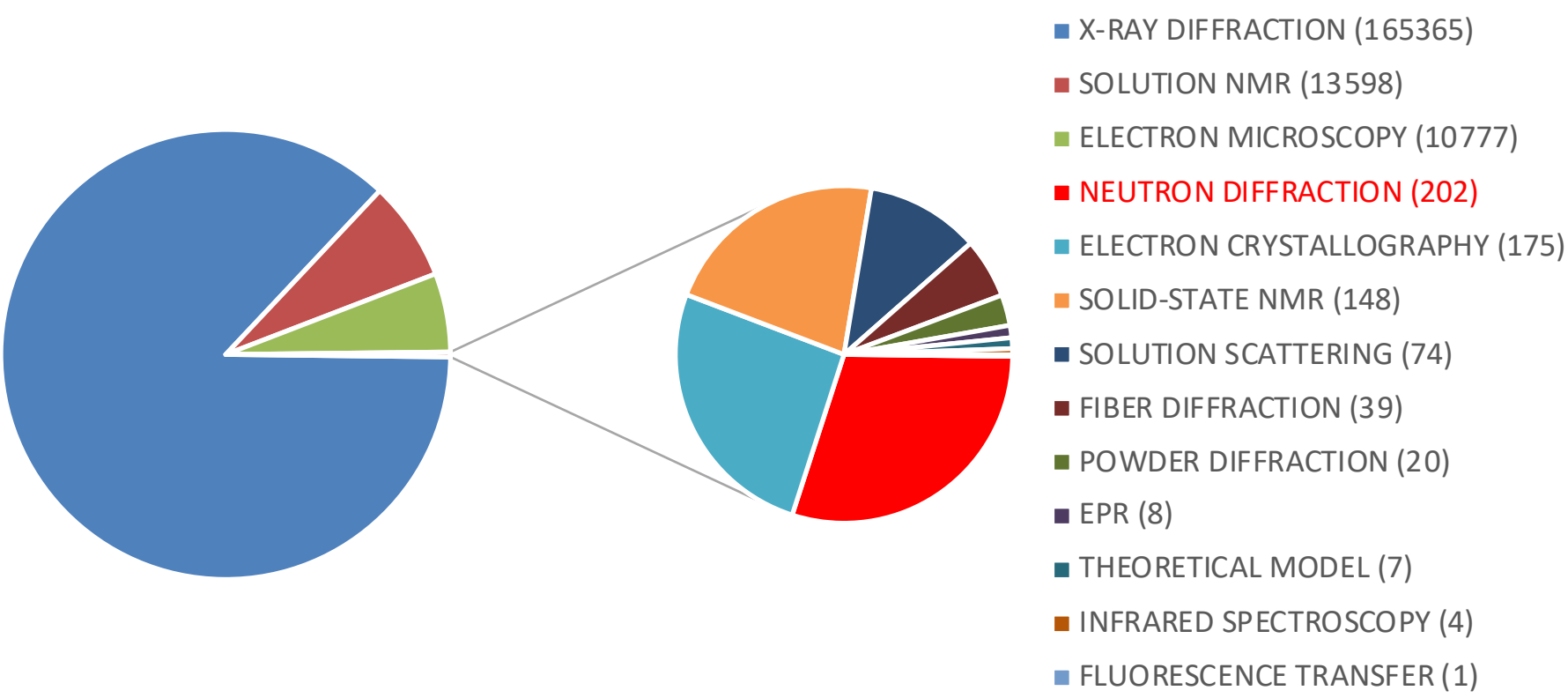

http://www.rcsb.org/

Total number of structures: 190418

X-ray data versus neutron data on the same protein:

X-ray d_{min}= 1.5Å:

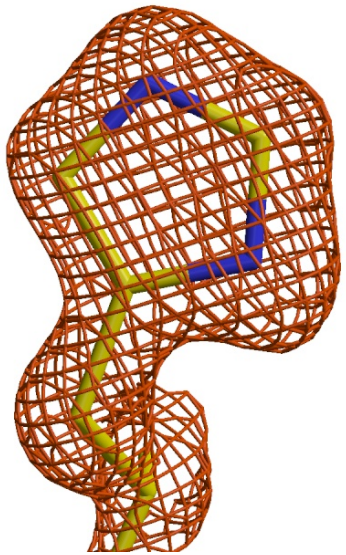

2Fo-Fc map; +1.5σ

neutrons d_{min}= 1.5Å:

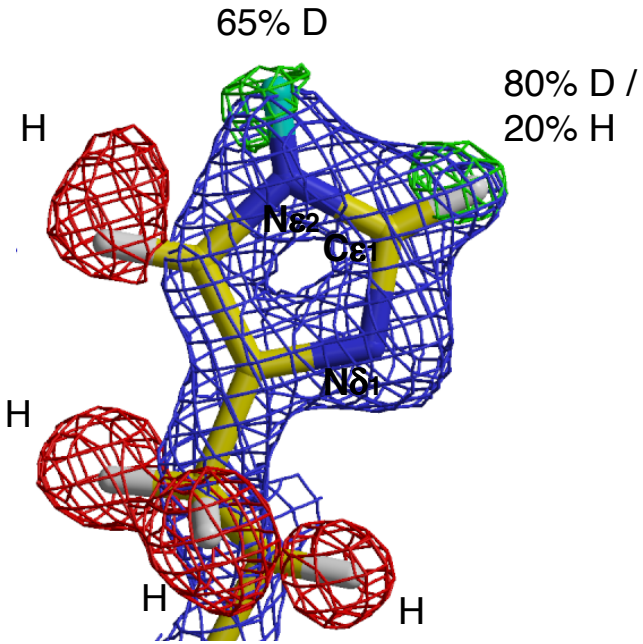

2Fo-Fc map; +1.5σ

Fo-Fc omit-map; -3.0σ

Fo-Fc omit-map; +3.0σ

Niimura N, Chatake T, Ostermann A, Kurihara K, Tanaka T. (2003) Z. Kristallogr. 218:96

Introducing: The free neutron

- udd particle with magnetic moment, decays to proton and anit-electron neutrino with half life time of 611 s.

m_n= 1.008665 atomic units
μ_n= –1.913 μ_N (nuclear magnetons)
Charge q_n= (1.5 ±2.2) x 10^{-22} proton charge; i.e. ~ zero
Electric dipole moment < 6 x 10^{-25}e-cm, i.e. zero

Ways to produce free neutrons for scattering applications:

- Fission of Uranium 235 in nuclear reactors
- Spallation: Shooting 3 GeV protons on Tungsten
- Nuclear reactions: (p,n) processes, some MeV Protons needed
- Natural decay of some elements: Californium sources

Neutrons are scattered by the nuclei, x-rays by the electron shells of the atoms

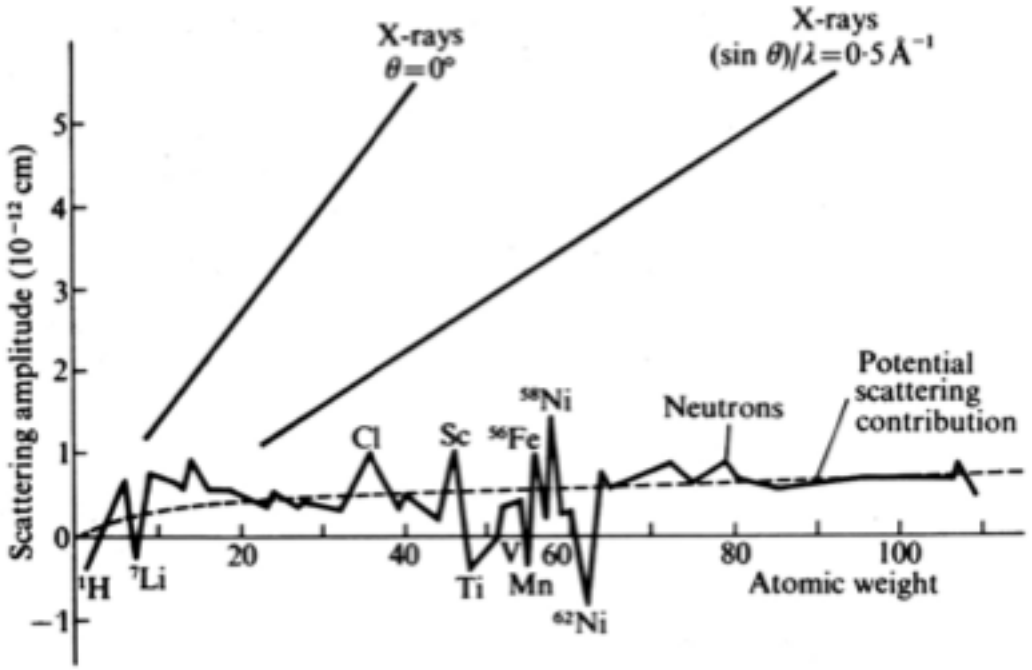

FIG. 22. Irregular variation of neutron scattering amplitude with atomic weight due to superposition of 'resonance scattering' on the slowly increasing 'potential scattering'; for comparison the regular increase for X-rays is shown. (From *Research* (*London*) 7, 257 (1954).)

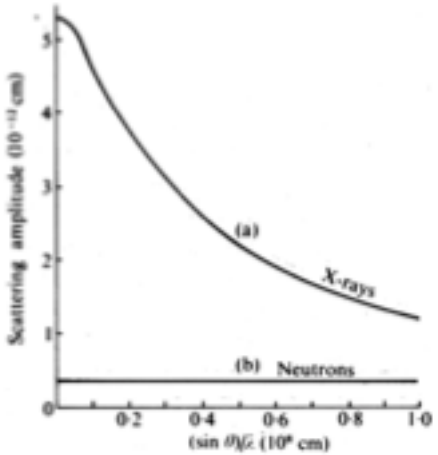

FIG. 16. X-ray and neutron scattering amplitudes for a potassium atom.

Atoms are point-like particles for neutrons, but for x-rays the electron shell shows some extension on the scale of the atom distances.

The neutron deBroglie wavelength is linked to its speed: $\lambda = \frac{h}{mv}$

2 Å neutrons travel with 2000 m/s and have an energy of 20 meV

Advantages of structure determination with neutrons:

Comparison of form factors (X-ray) and scattering lengths (neutrons):

Nucleus	atomic number	scattering length [10^{-12} cm]
^{1}H	1	**-0.378**
^{2}H	1	**0.667**
^{12}C	6	**0.665**
^{15}N	7	**0.921**
^{16}O	8	**0.581**

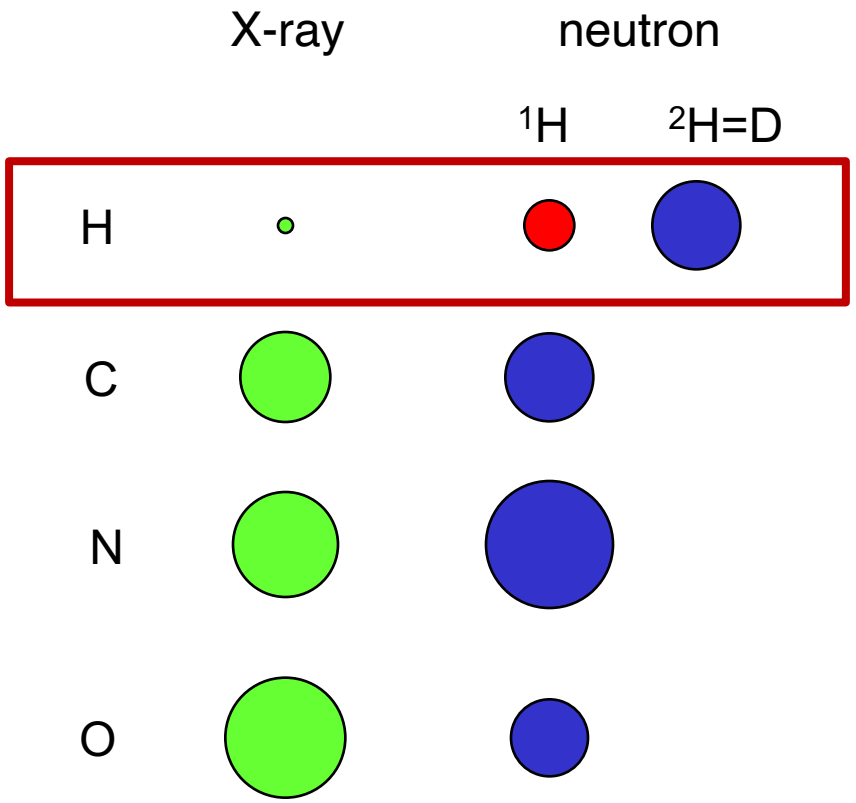

diameters correspond to:
form factor / scattering length
(scaled for C-atom)

σ_{coh} of ^{1}H is 1.8×10^{-28} m^2 but
σ_{incoh} of ^{1}H is 80.2×10^{-28} m^2
Large background from hydrogen atoms!

Advantages of Structure Determination with Neutrons

Hydrogen/deuterium atoms can be resolved even at a resolution of $d_{min} \approx 2.5$ Å (for ^2H). Therefore one can determine:

- protonation states of amino acid side chains and ligands
- deuterium exchange as a measure of flexibility and accessibility (discrimination between **H** / **D**)
- solvent structure including hydrogen atoms

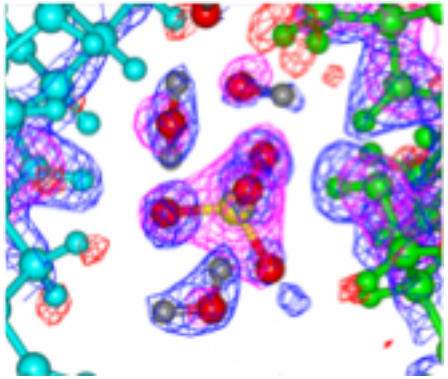

Water network in the contact region between two myoglobin molecules in the crystal.

x-ray map (magenta): contour level of +2.7σ
nuclear map (red): contour level of -1.75σ
nuclear map (blue): contour level of +2.3σ

Much less radiation damage as compared to x-rays: Metallo-proteins can be measured without reducing the metal centres

Neutron Protein crystallography

Crystallography: Overiew over the process

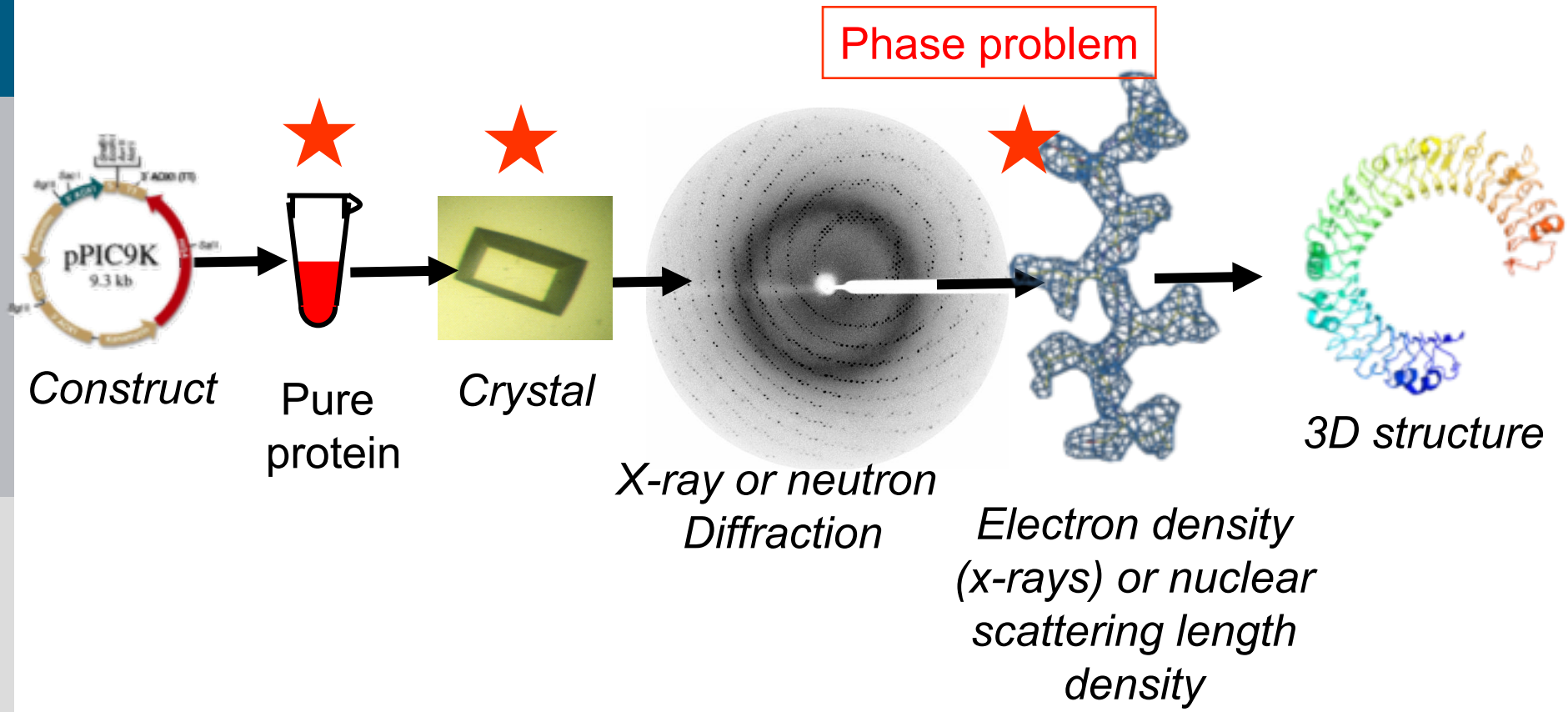

Harma Brondijk, Crystal and Structural chemistry, Utrecht University

Size considerations of protein crystals

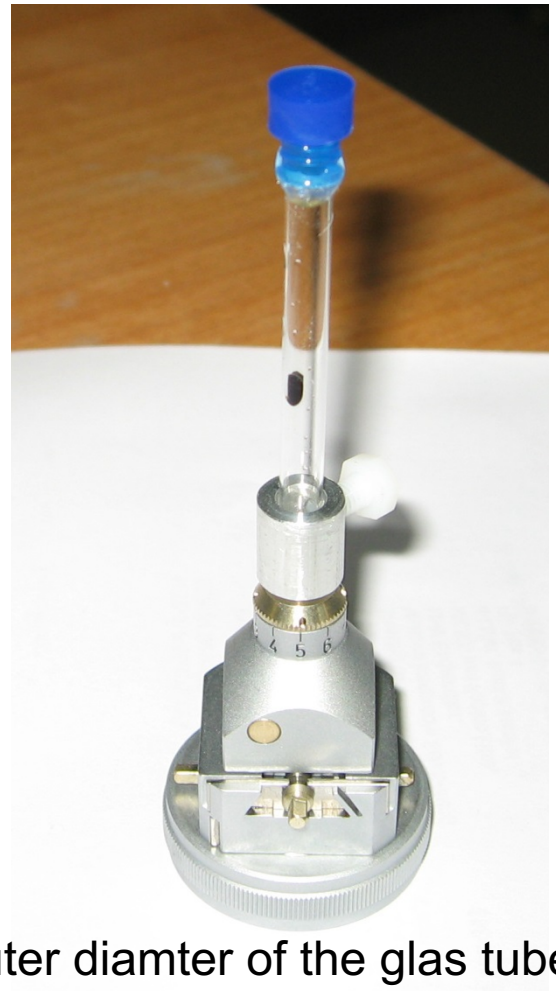

size:
x-ray-crystallography:
ca. 10 µm x 10 µm x 10 µm
typically cryoprotectants needed to facilitate measurements at low (80 K) temperatures

neutron protein crystalography:
The desirable size should be around
1 mm x 0.5 mm x 0.5 mm (depending on the protein/space group)

Outer diamter of the glas tube: 5 mm

Cryo-mounting of large crystals

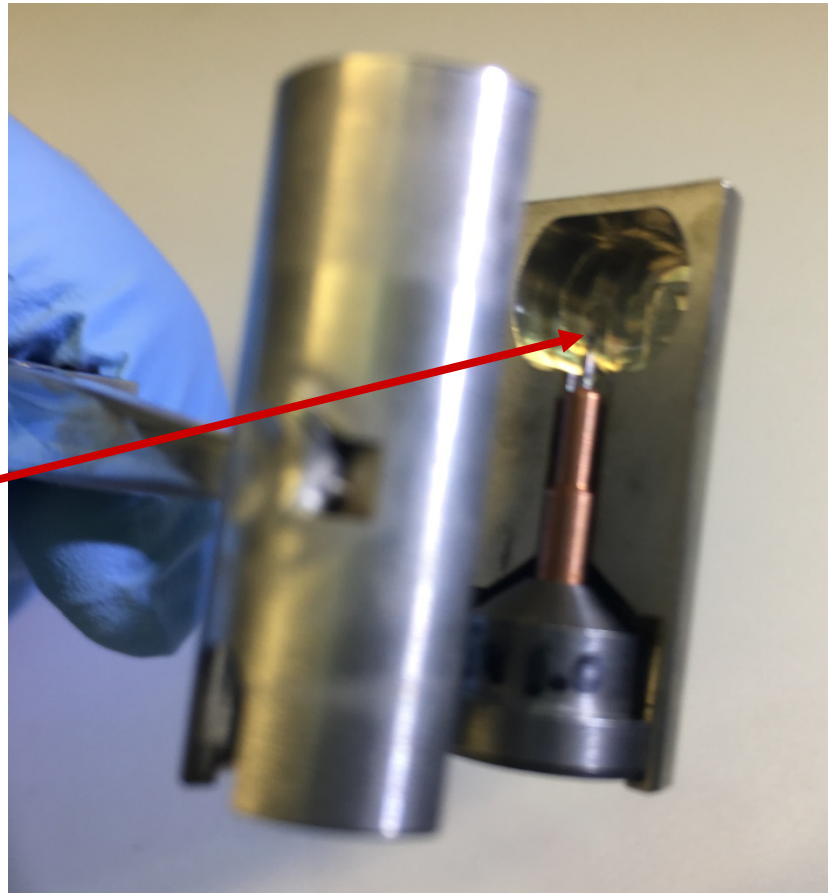

- Avoid hydrogenated polymers in the loop, use capton (Mitigen) or carbon meshes instead (especially when you have a fully deuterated protein)
- Make sure that your crystal fits into the cryoTong: We prefer the 18 mm one.

Schematic overview over BioDiff: A neutron protein diffractometer: collaboration between JCNS and TUM (FRM-II)

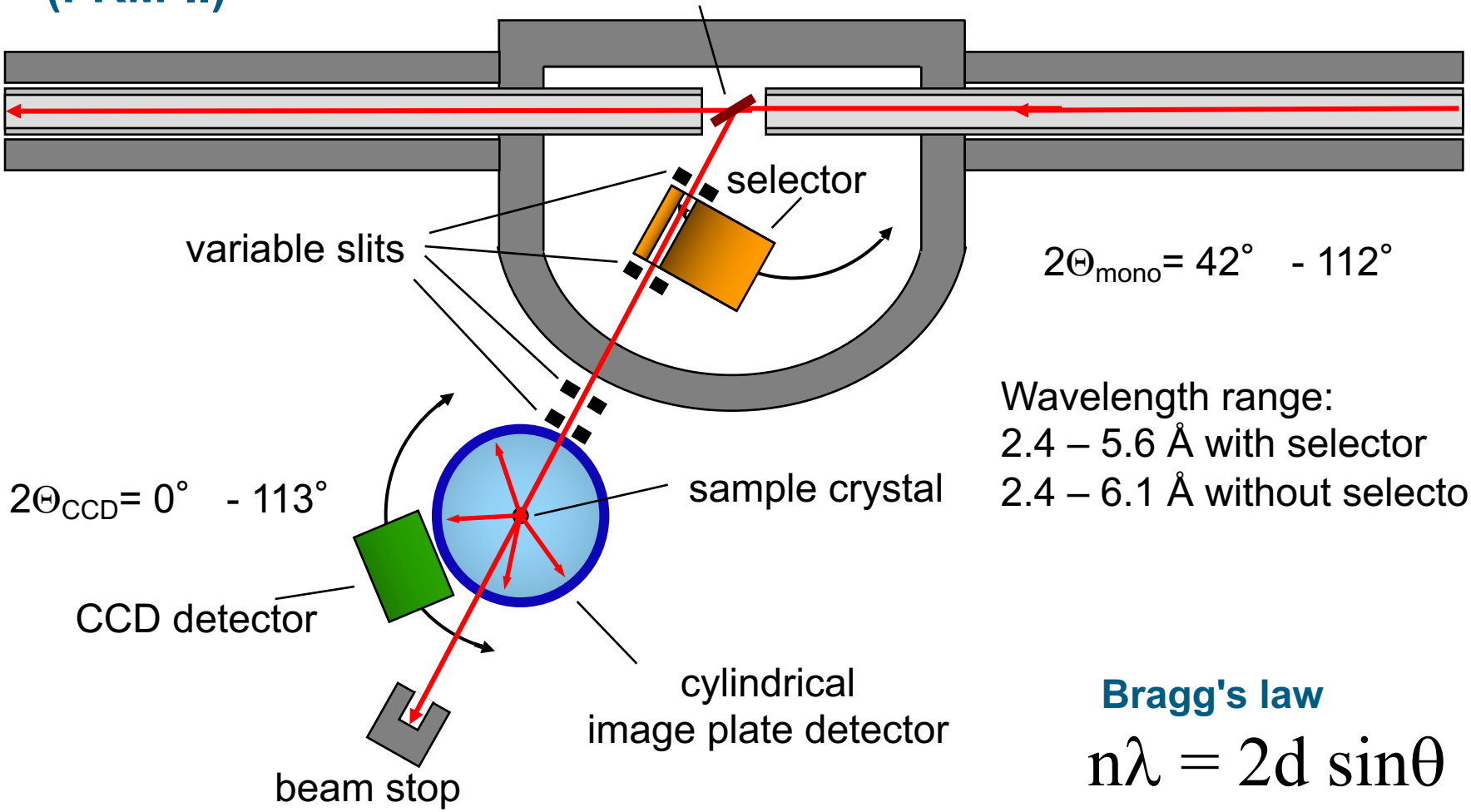

Wavelength range:
2.4 – 5.6 Å with selector
2.4 – 6.1 Å without selector

Bragg's law

$$n\lambda = 2d \sin\theta$$

BioDiff, the corresponding view in reality:

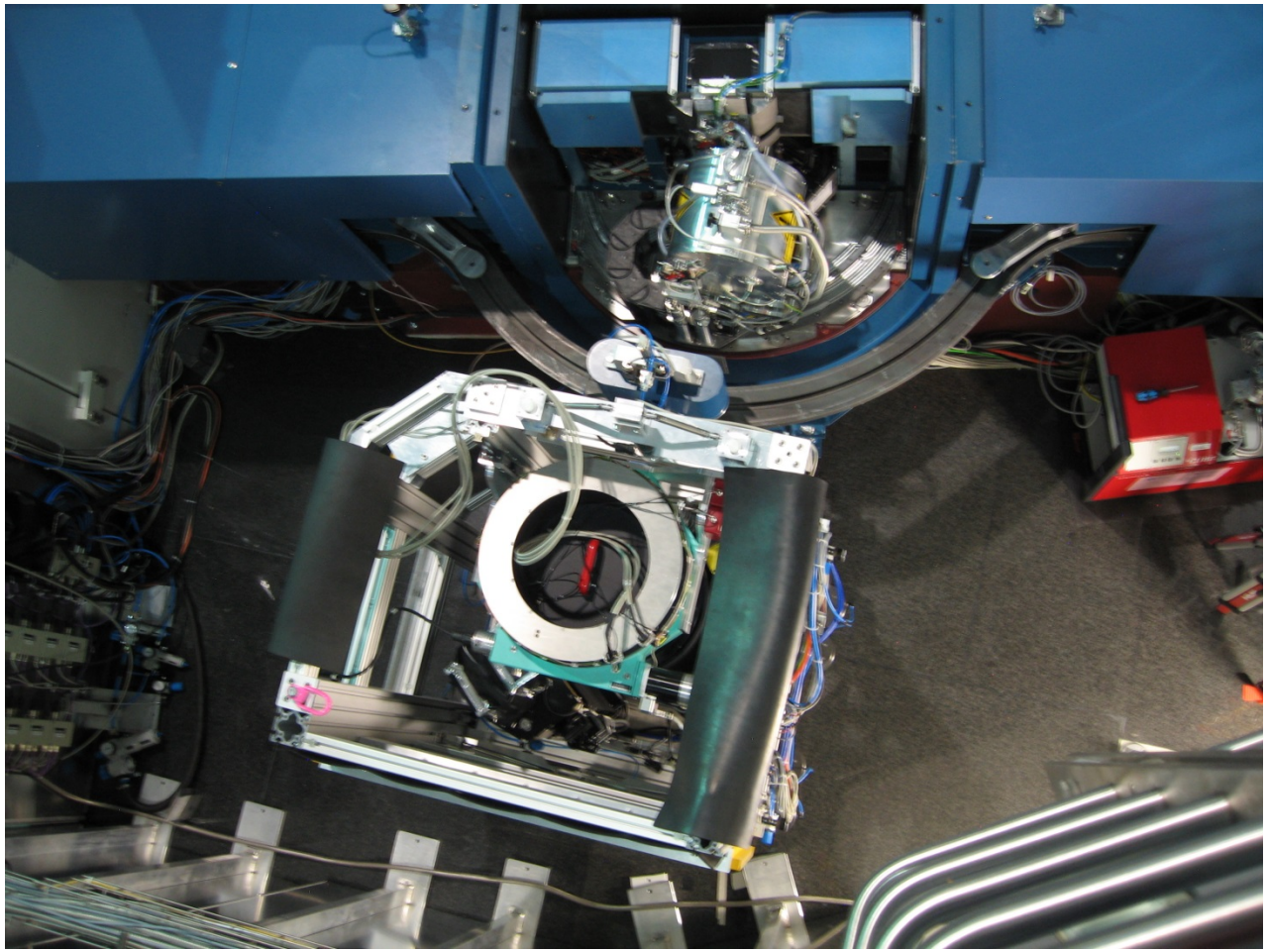

The Simultaneous Construction-phase in Garching and Jülich

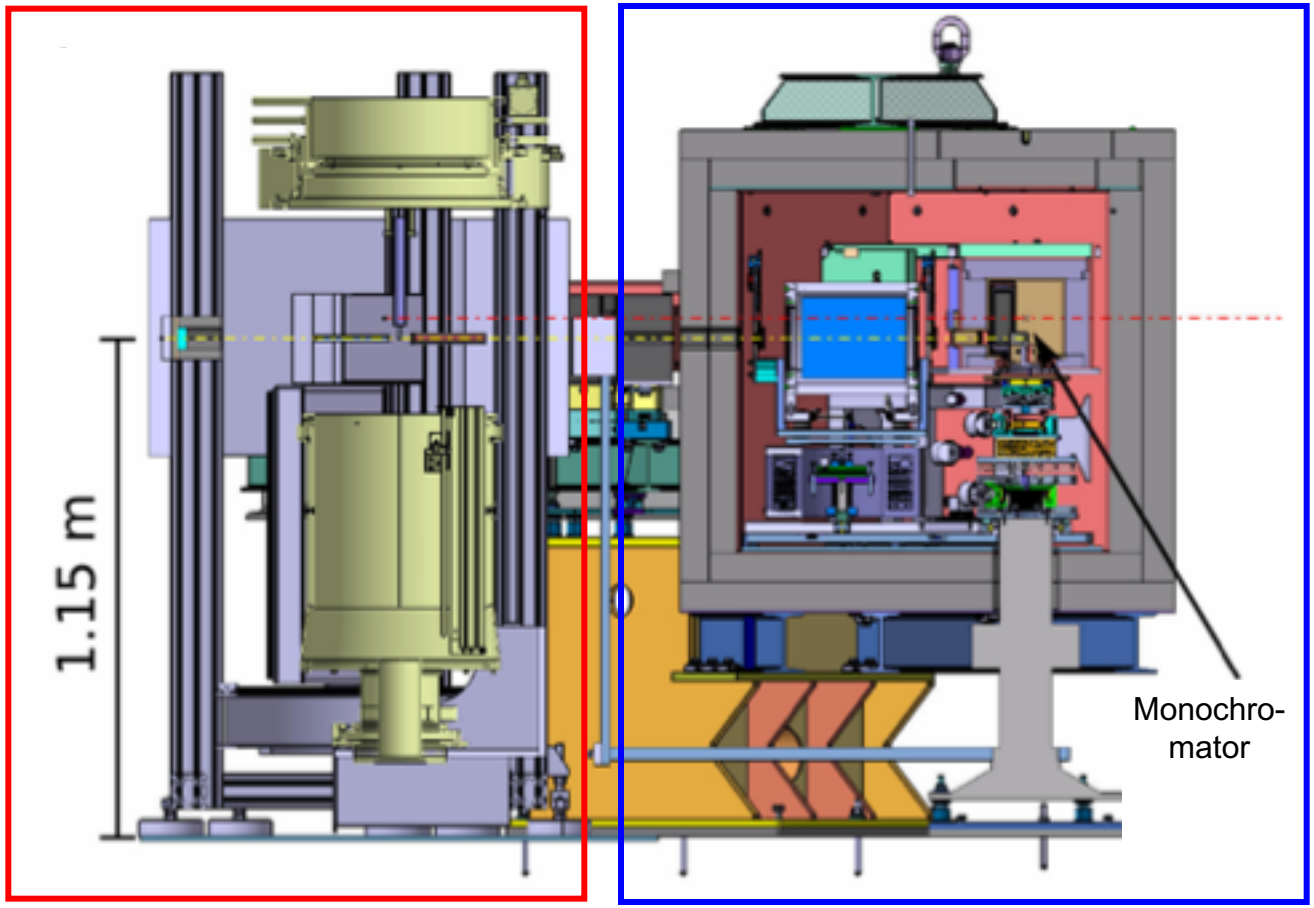

Detector unit, constructed and built in Garching (Ph. Jüttner, MLZ)

Monochromator-shielding, constructed and built in Juelich (B. Laatsch, ZEA-1 Engineering)

A Most Recent View of the Instrument BioDiff

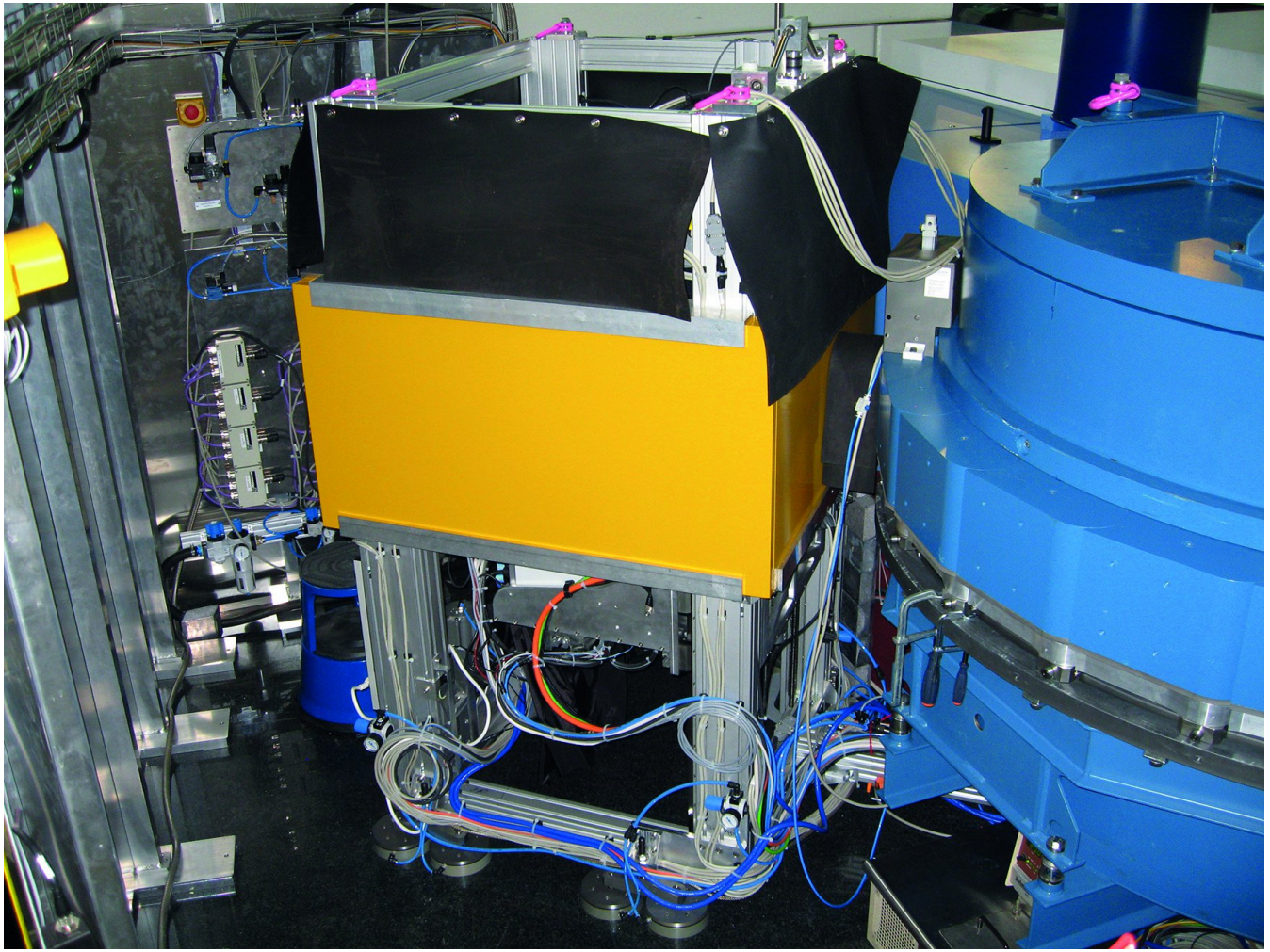

Myoglobin protein crystal (deuterated mother liquor) full data set recorded with CCD-camera

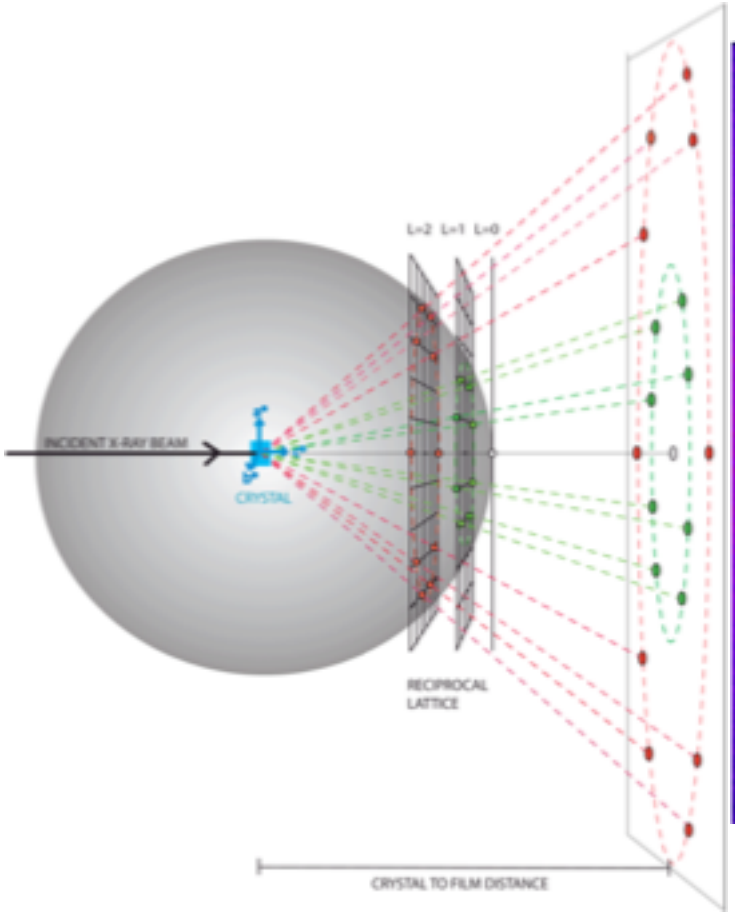

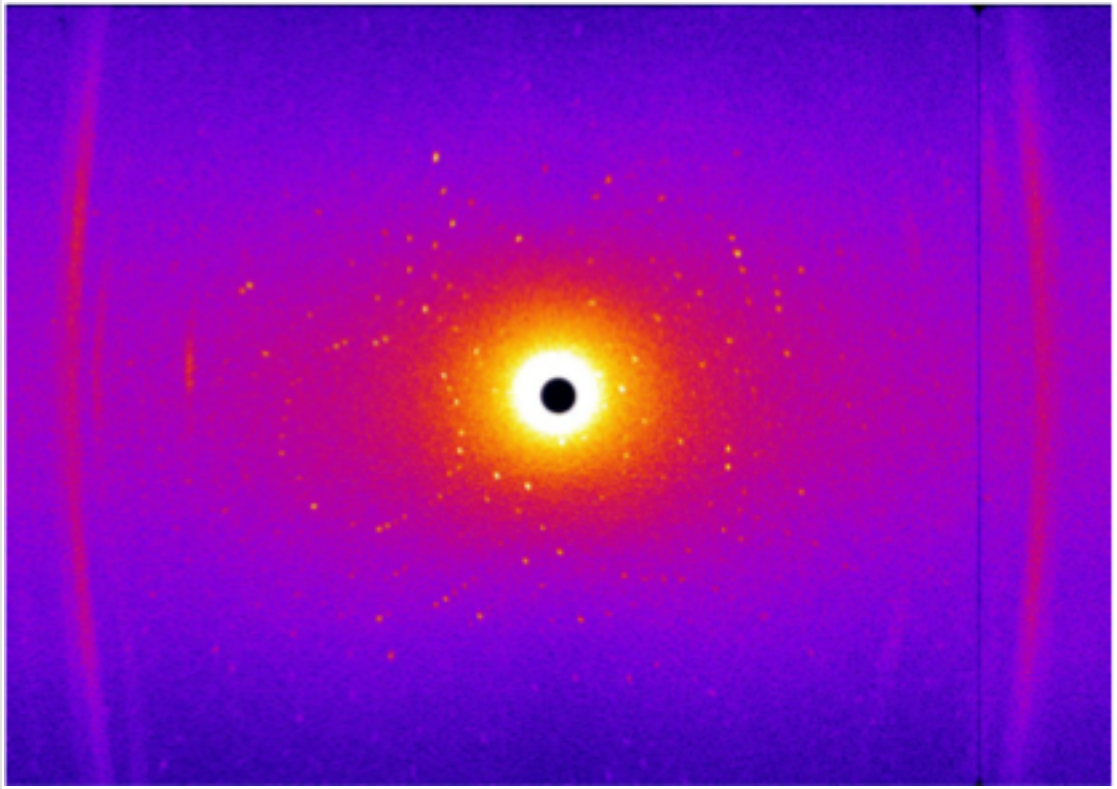

BioDiff: exposure time per frame: typically between 20 minutes and 4 hours.

The Two Detectors of BIODIFF

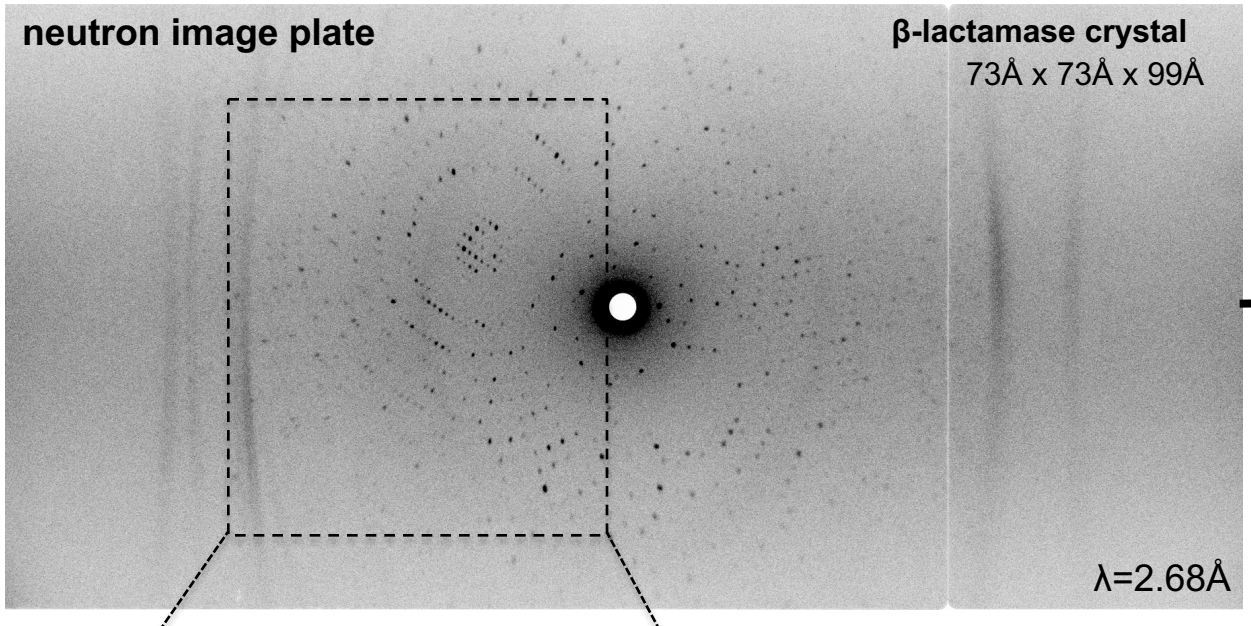

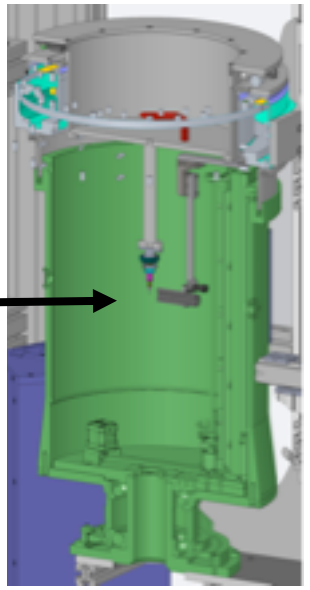

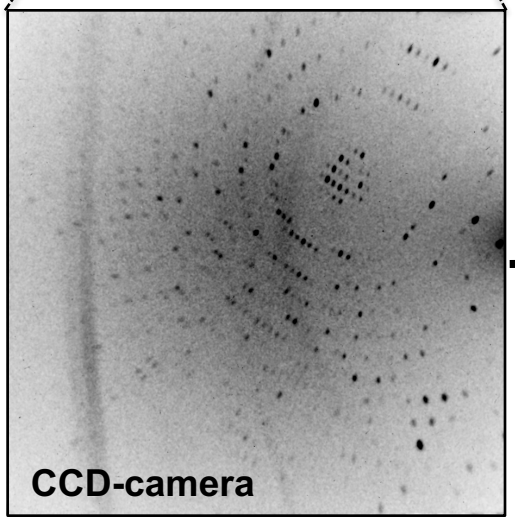

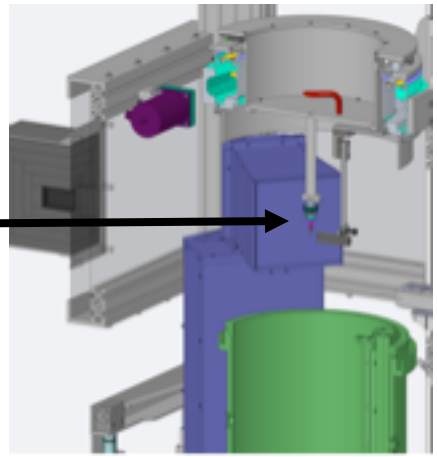

NIP-scanner

- larger solid angle
- readout time ≥ 4 min

CCD-camera

- smaller solid angle
- readout time ≥ 1 sec

Integration of partial Bragg peaks with the commercial software hkl-denzo up to d_{min}=1.5 Å

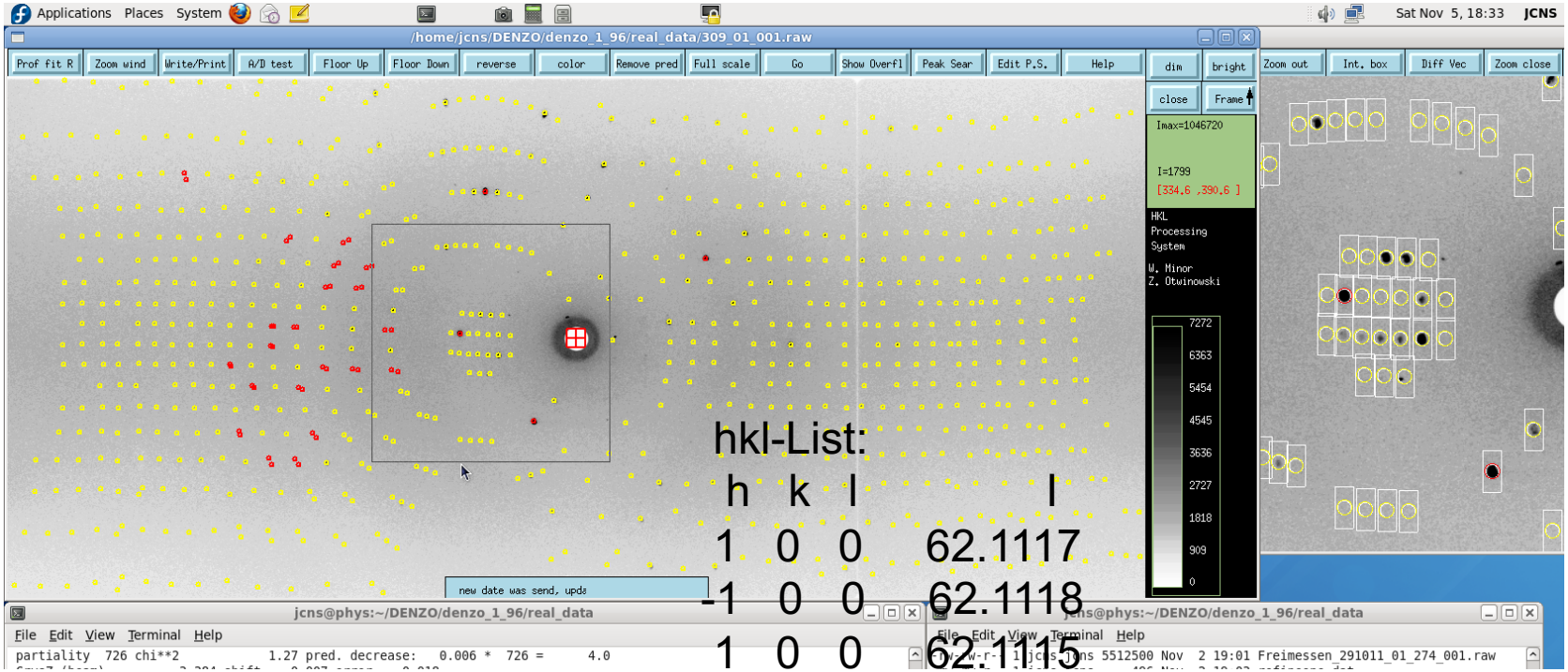

hkl-List:

h	k	l	I
1	0	0	62.1117
-1	0	0	62.1118
1	0	0	62.1115
-1	0	0	62.1120
0	0	-1	33.5555
1	0	-1	33.5589
0	0	1	33.5533
-1	0	1	33.5511

ca. 300 images

Flow chart of data treatment and model building

Scans at varying crystal orientation
Scan := Series of detector images

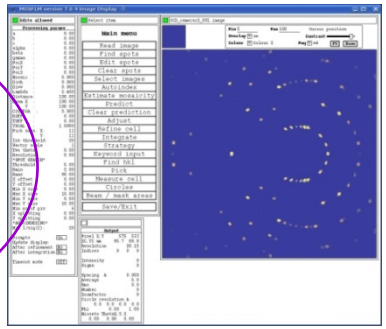

-MOSFLM
-HKL-denzo
- HKL2000
(comercial)

Data reduction

- determination of crystal orientation, unit cell dimensions etc.
- Calculating integral of reflection intensities

hkl-list for each scan:
h k l Intensity Intensity error

Scaling of each hkl list to match each other

-SCALA (CCP4-program package)

Unified hkl-list of measurement := complete data set

Calculation of a first map

Additional information from the solution of the phase problem

Structure refinement

-Refinement of atom coordinates displacements
- Calculation of scattering density maps (netrons) or electron density maps (x-rays)

Map-plotting

- inspection of model to fit the map)
- real space changes and refinement to the model

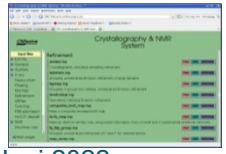

-nCNS
-PHENIX

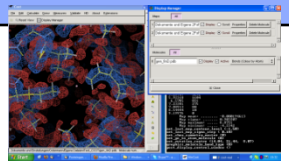

-XtalView
-Coot

Application Example of neutron protein crystallography: Research on Corona Virus proteins from SARS-COV-2 with x-ray and neutron crystallography

How does the virus look like?

The size is 60-160 nm

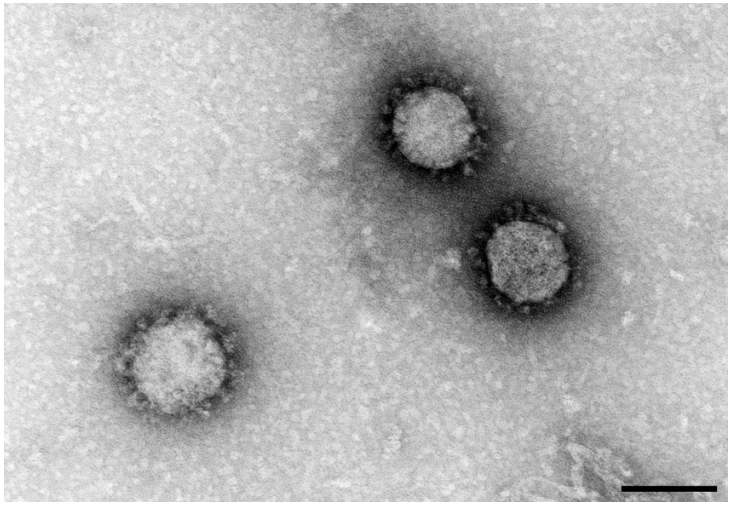

Scale bar = 100 nm,
Source: RKI web-site,
Source: *Hans R. Gelderblom, Freya Kaulbars/RKI*

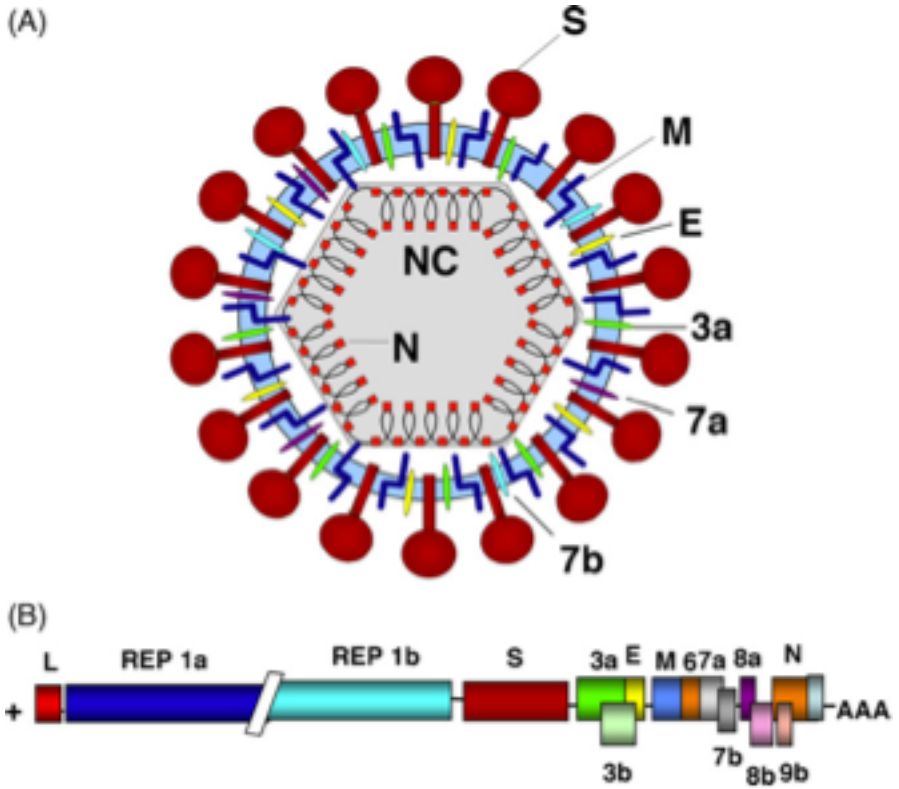

Fig. 2. Structure and genome organization of SARS-CoV. (A). Schematic diagram of SARS-CoV structure. S, spike protein; M, membrane protein; E, envelope protein; N, nucleoprotein; 3a, 7a, and 7b, structural proteins of SARSCoV. (B). Representation of a prototype SARS-CoV genome. Poly(A) tail is indicated by AAA. Numbers and letters indicate viral genes.: Virus Research 133 (2008) 45–62

How does it work?

It programms a human cell to produce replicas of it:

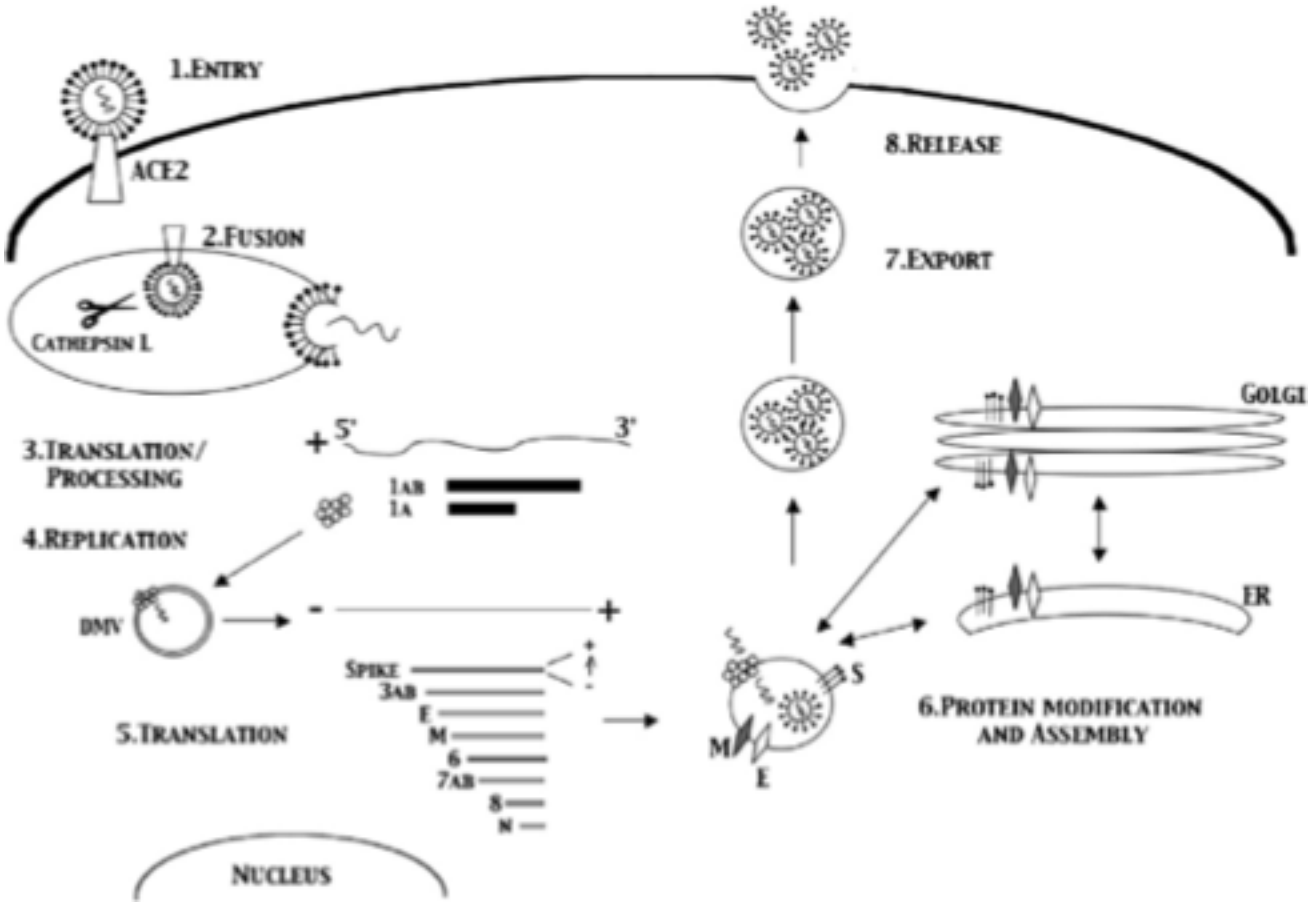

Virus Research 133 (2008) 101–112

The genome and the encoded proteins of SARS-CoV-2

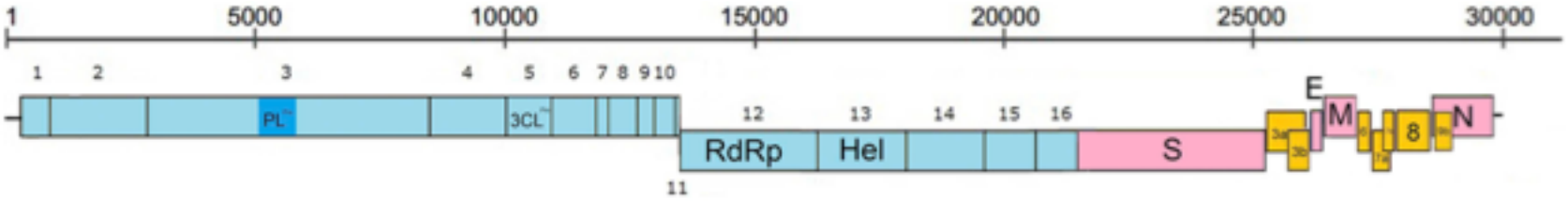

Fig. 1. Genome organization of SARS-CoV. ORF1ab with nsp1–16 are colored in blue. Structural proteins including S, E, M and N are in pink. Accessory proteins were
numbered and in yellow. (For interpretation of the references to colour in this figure legend, the reader is referred to the web version of this article.)

Main protease cleaves viral proteins to the right length: This is why it is an important drug target.

From: Infection, Genetics and Evolution 71 (2019) 21–30

The main protease of the corona virus

Here, an inhibitor is bound to the protein

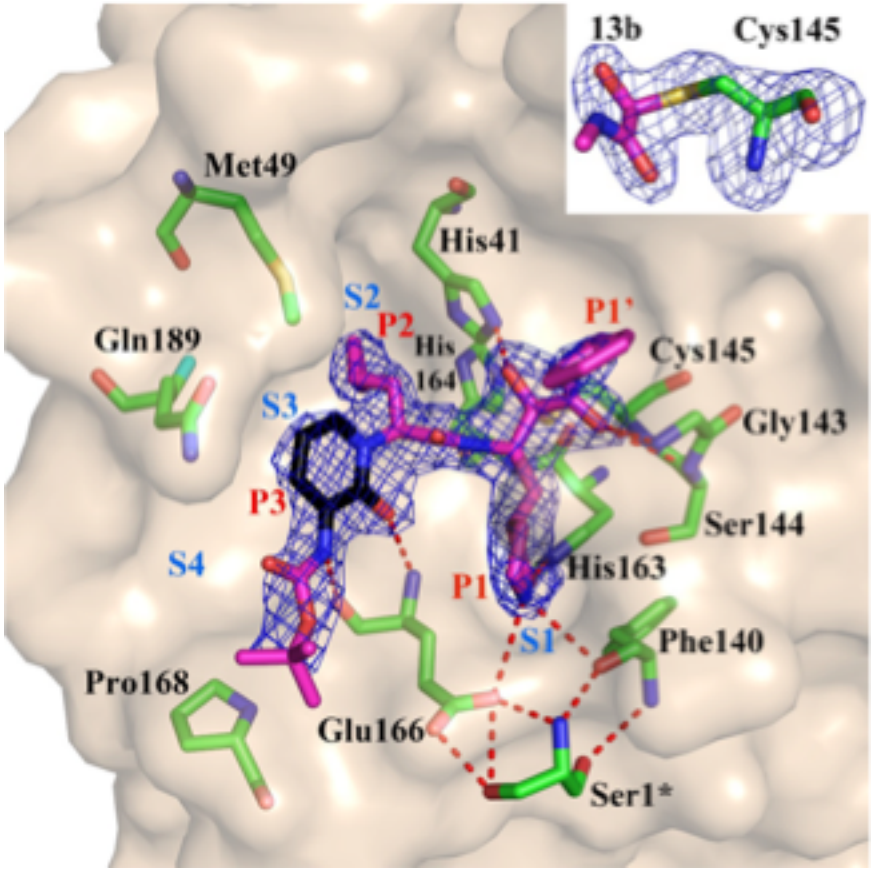

L. Zhang *et al*., *Science* 10.1126/science.abb3405 (2020).

Fig. 3. Compound 13b in the substrate-binding cleft located between domains I and II of the Mpro, in the monoclinic crystal form (space group C2). Fo-Fc density is shown for the inhibitor (contouring level: 3σ). Carbon atoms of the inhibitor are magenta, except in the pyridone ring, which is black; oxygen atoms are red, nitrogens blue, and sulfur yellow. Light-blue symbols S1, S2, S3, S4 indicate the canonical binding pockets for moieties P1, P2, P3, P4 (red symbols) of the peptidomimetic inhibitor. Hydrogen bonds are indicated by dashed red lines. Note the interaction between the N-terminal residue of chain B, Ser1*, and Glu166 of chain A, which is essential for keeping the S1 pocket in the right shape and the enzyme in the active conformation. Inset: Thiohemiketal formed by the nucleophilic attack of the catalytic cysteine onto the α-carbon of the inhibitor in its Fo-Fc density (contoured at 3σ). The stereochemistry of the α-carbon is *S*. See fig. S8 for more details.

The first neutron structure solved for the main protease in its apo state (empty binding pocket)

A: X-ray data

B: neutron data

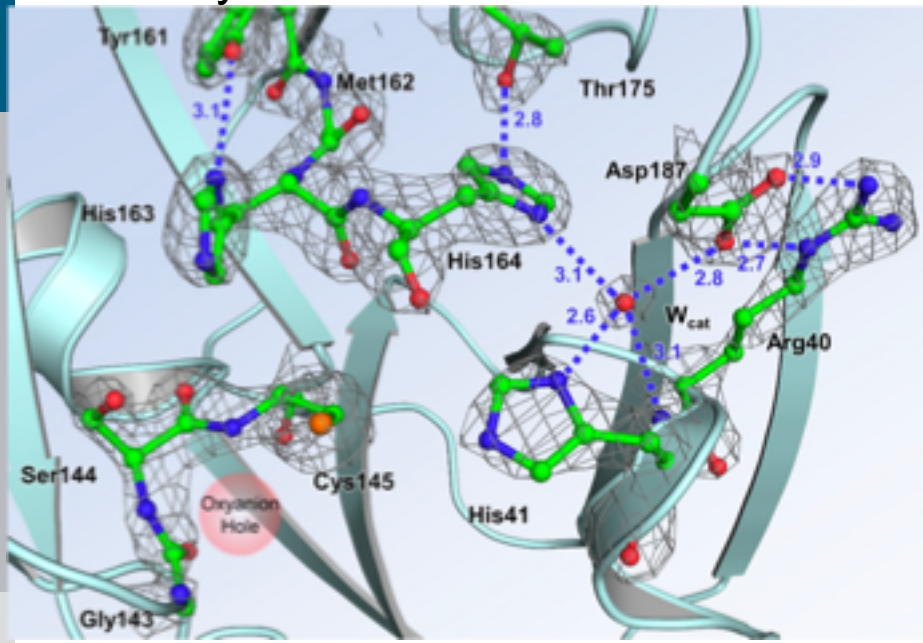

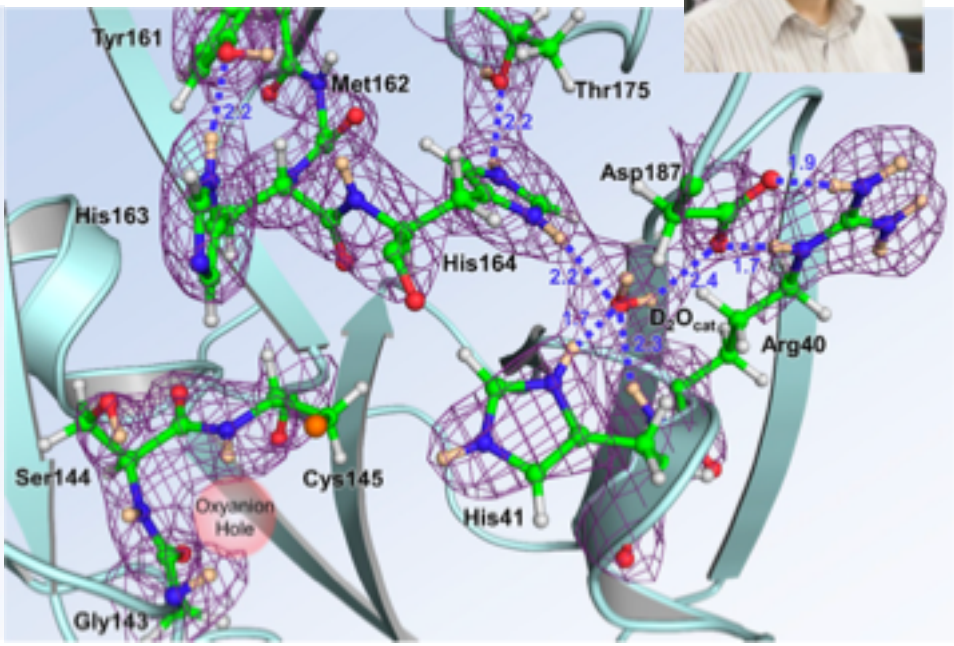

Figure 3. The catalytic site of SARS-CoV-2 3CL Mpro. (**A**) The 2FO-FC electron density map contoured at 2.0 σ level (grey mesh) with no hydrogen atoms visible. Distances between the heavy atoms in Ångstroms illustrate possible hydrogen bonds. (**B**) The 2FO-FC nuclear density map contoured at 2.0 σ level (violet mesh), allowing visualization of the actual protonation states and hydrogen bonding interactions (D…O distances are shown in Ångstroms).

From: https://www.biorxiv.org/content/10.1101/2020.09.22.308668v1, data measured at MANDI and IMAGINE at Oak Ridge National Lab, Oak Ridge, Tennessee, USA

His41: doubly protonated
Cys145: deprotonated

Small angle neutron Scattering (SANS)

And now the low resolution...

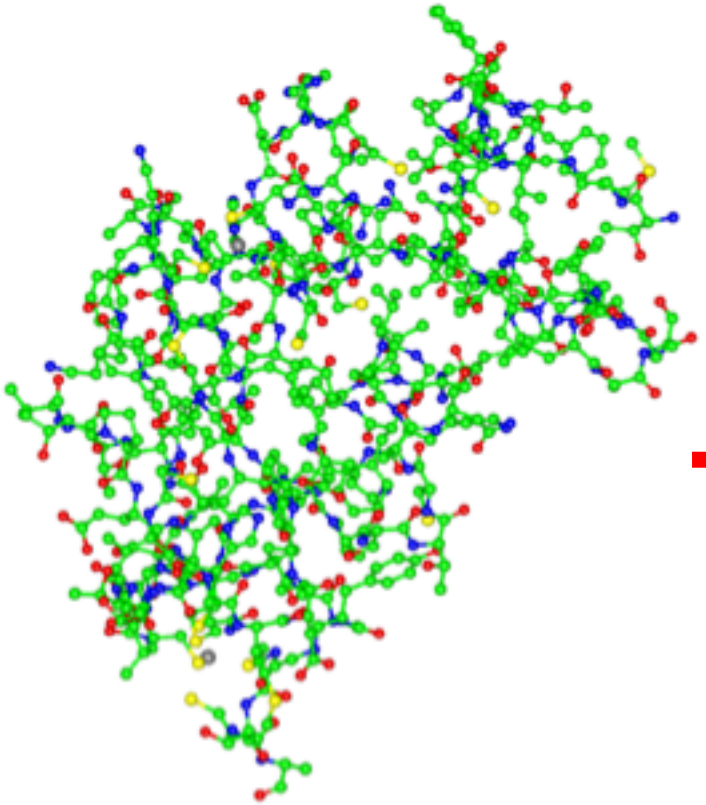

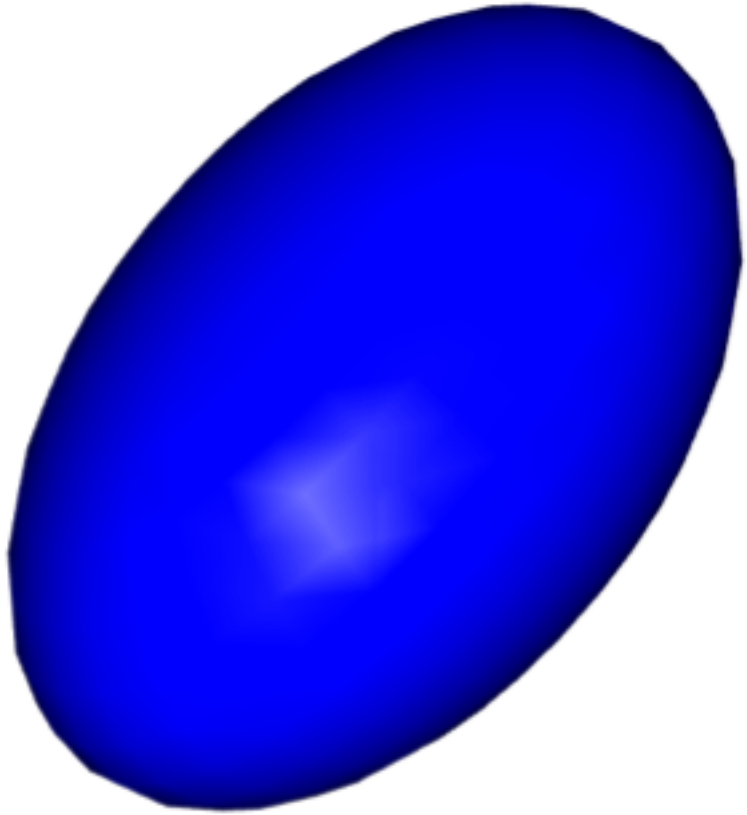

nsp10 of SARS-CoV2, 6zct.pdb

Single crystal diffraction

Small angle neutron scattering (SANS)

Small angle neutron scattering

„Pinhole SANS“

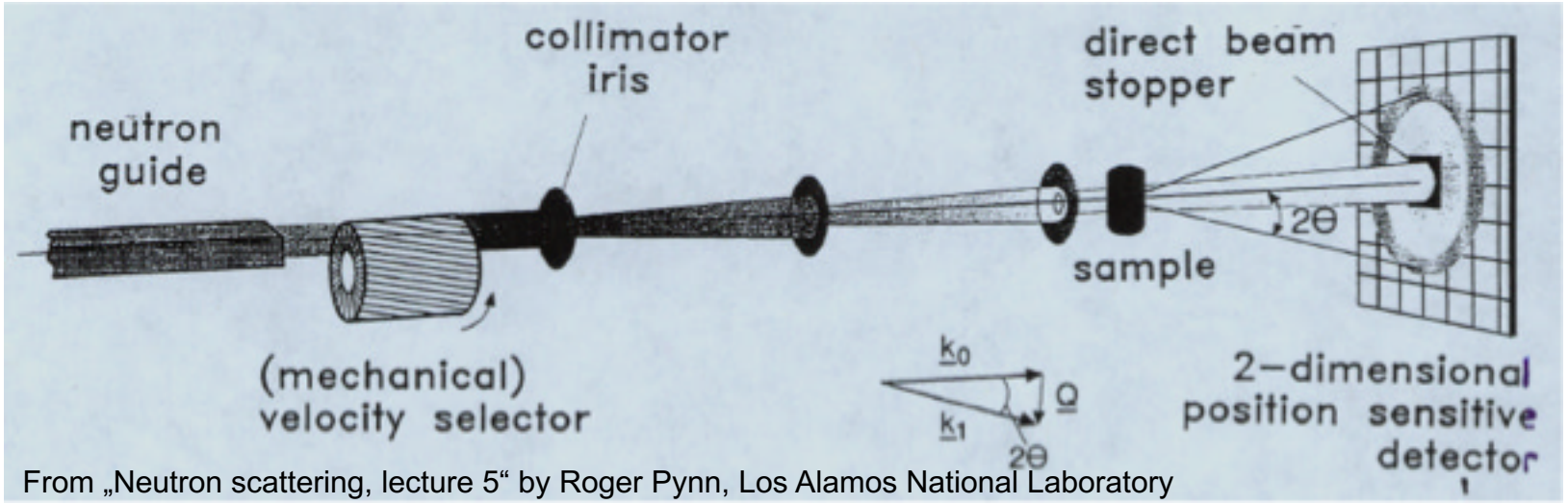

From „Neutron scattering, lecture 5“ by Roger Pynn, Los Alamos National Laboratory

„radial averaging“

$$\frac{d\Sigma}{d\Omega}(\mathbf{q}) = \frac{N}{V}\frac{d\sigma}{d\Omega}(\mathbf{q}) = \frac{1}{V}\left|\int_V \rho(\mathbf{r})e^{i\mathbf{q}\cdot\mathbf{r}}d\mathbf{r}\right|^2$$

„Rayleigh-Gans Equation“

Form factor of a sphere

For a sphere of radius r

$$P(q) = \left[\frac{3(\sin(qr) - qr\cos(qr))}{(qr)^3}\right]^2$$

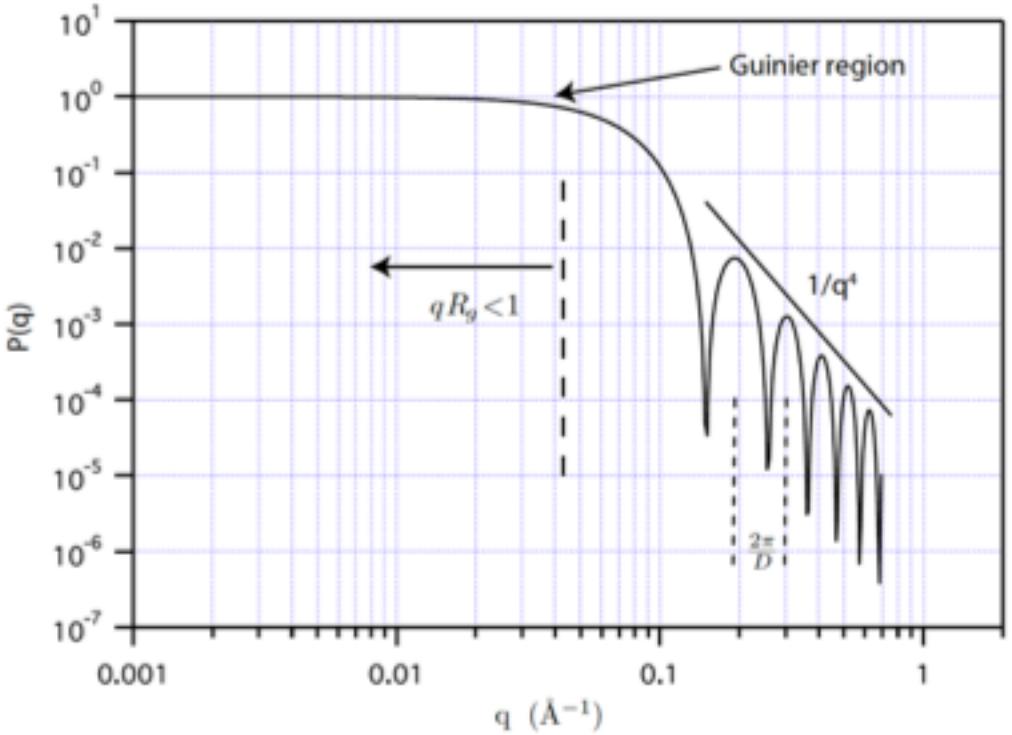

Figure 7: Form Factor spheres of radius 3Å. $R_g =$ 2.3 Å $\qquad R_g^2 = \frac{3}{5}R^2$

Figure taken from „Introduction to Small-Angle Neutron Scattering and Neutron Reflectometry“, Andrew J Jackson, NIST Center for Neutron Research, May 2008

Contrast matching

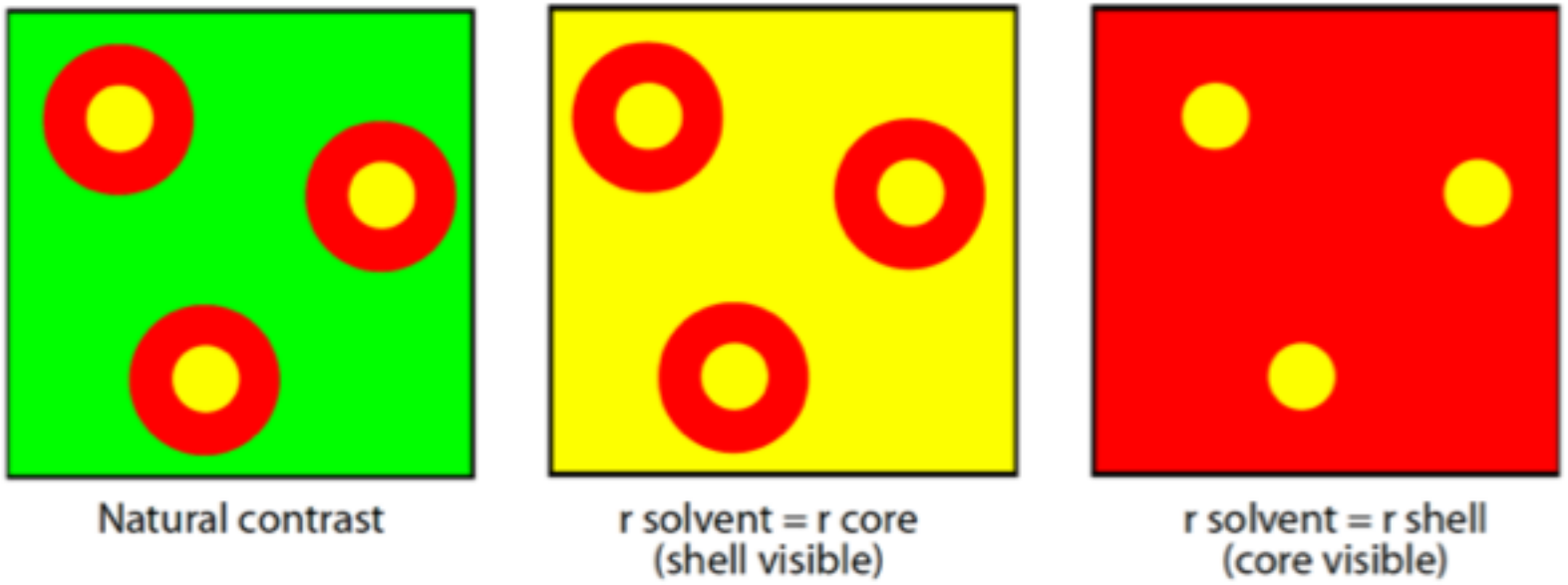

Figure 9: The effect of contrast variation on the measurable structure of a core-shell particle

Figure taken from „Introduction to Small-Angle Neutron Scattering and Neutron Reflectometry“, Andrew J Jackson, NIST Center for Neutron Research, May 2008

Contrast matching in water solutions

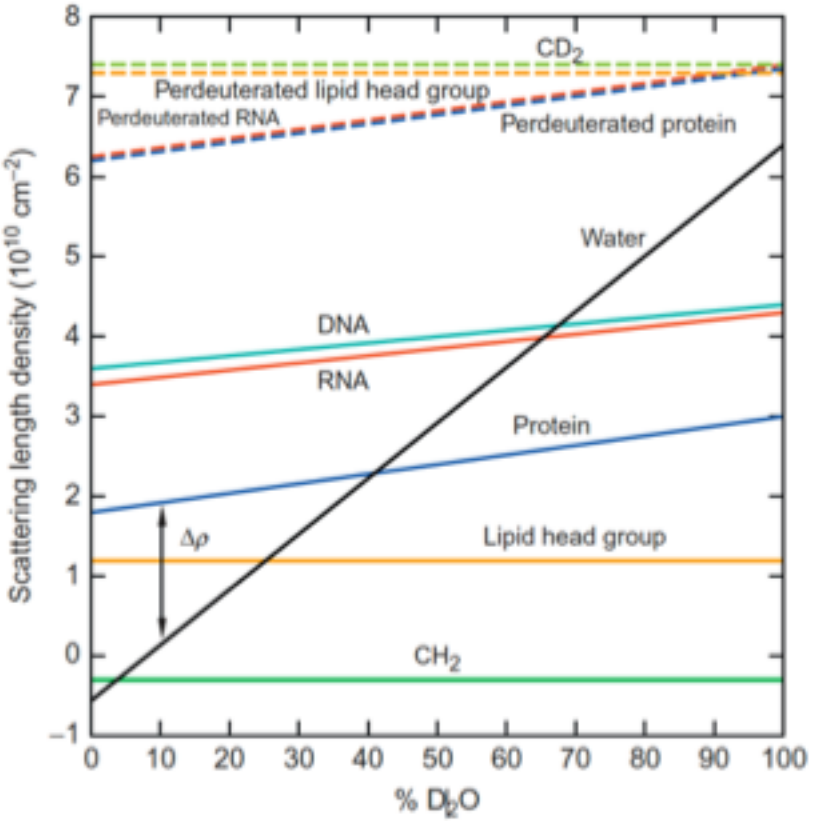

Figure 1 Plot of the neutron scattering length density versus % D_2O in the solvent for water compared to those for protein, RNA, DNA, and the components of lipids (lipid head group and CH_2), along with their perdeuterated counterparts.

From: Methods in Enzymology, Volume 566, p. 159, 2016

One application example of contrast matching SANS

Problem: How to measure the structure of a membrane protein in its most natural environment?

Sophie Combet

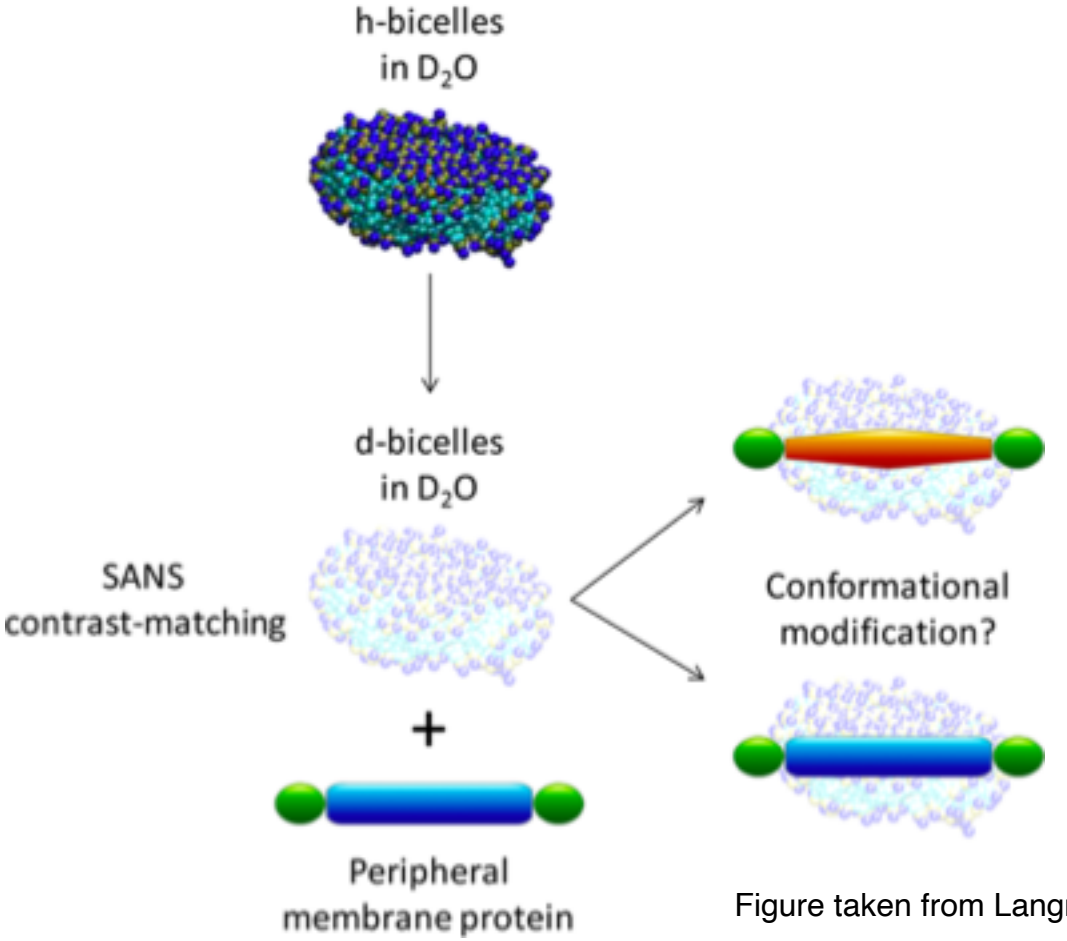

Figure taken from Langmuir 2017, 33, 6572

Idea: Put a bicelle around it and match it with a mixture of deuterated and hydrogenated lipids to 100% D_2O

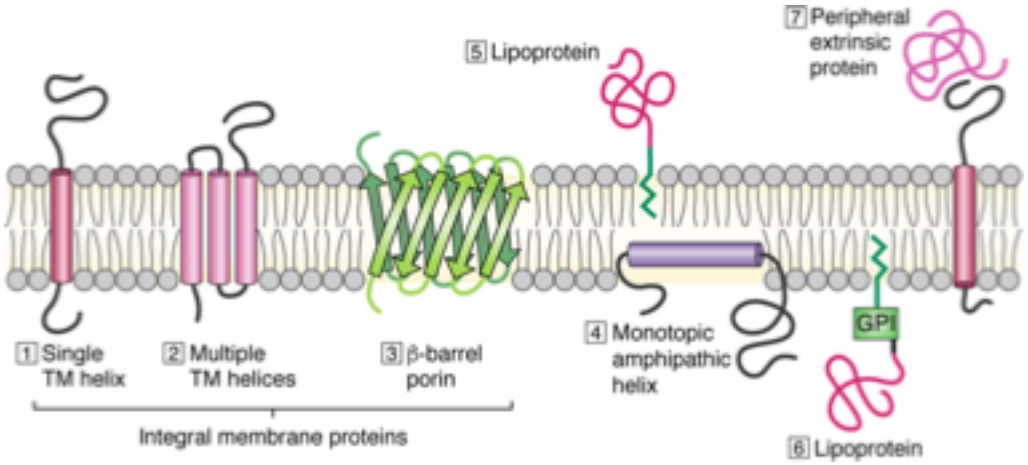

Classification of membrane proteins

Figure taken from J. Biol. Chem. (2019) 294(44) 15914

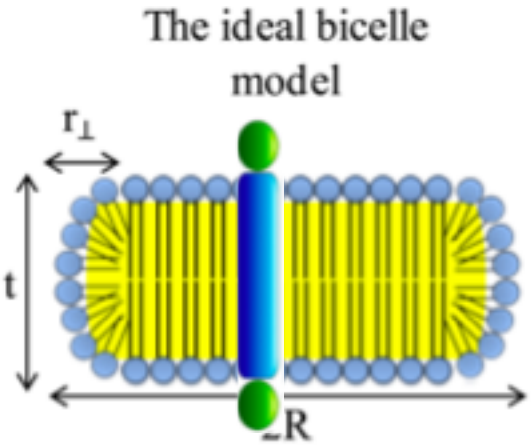

Figure 1. (A) Schematic representation of the ideal bicelle model. For DMPC/DHPC bicelles, R is the radius of the bicelle, r⊥ is the thickness of the rim (11 Å, the length of a DHPC molecule), and t is the thickness of the DMPC bilayer (assumed to be 40 Å).

Figure taken from Langmuir 2017, 33, 6572

Bicelles are virtually invisible at 100%. D_2O buffer (d-TNE)

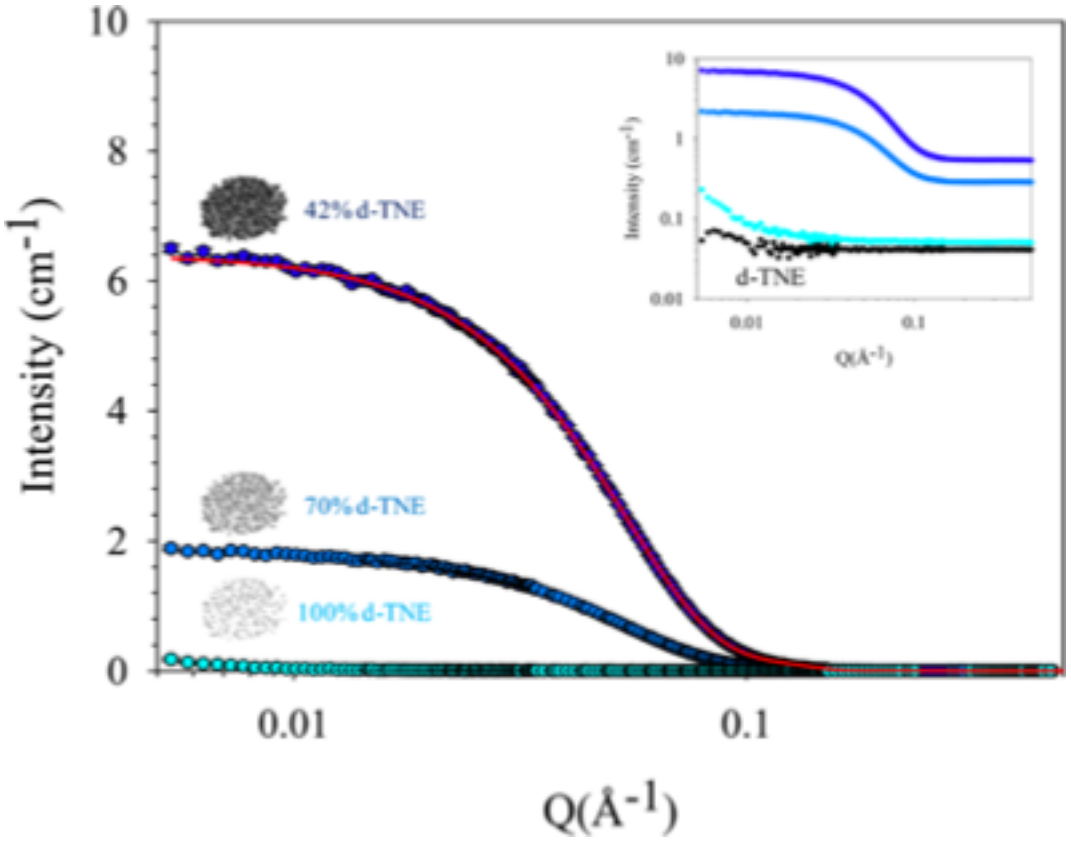

d-TNE buffer solution (20 mM Tris-d11, 150 mM NaCl, and 0.1 mM EDTA-d16, pD 7.5)

Figure taken from Langmuir 2017, 33, 6572

Only scattering from the protein is visible

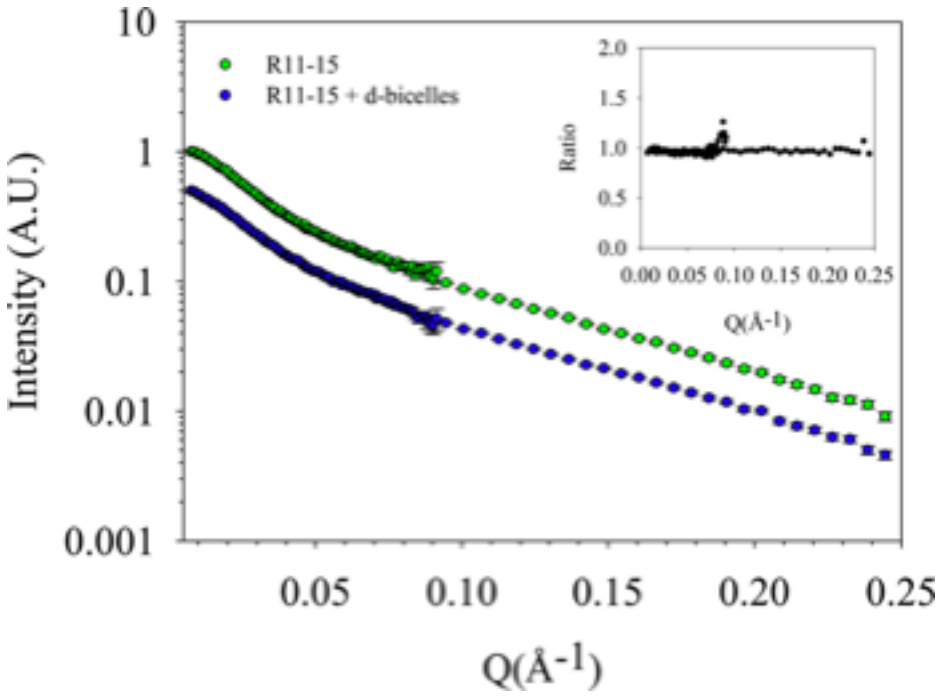

protein fragment belonging to the dystrophin central domain
DYS R11–15 (from the 11th to the 15th spectrin-like repeats)
= a well known very rigid protein

Figure taken from Langmuir 2017, 33, 6572

All neutron instruments can be sorted according to their energy resolution and type of scattering

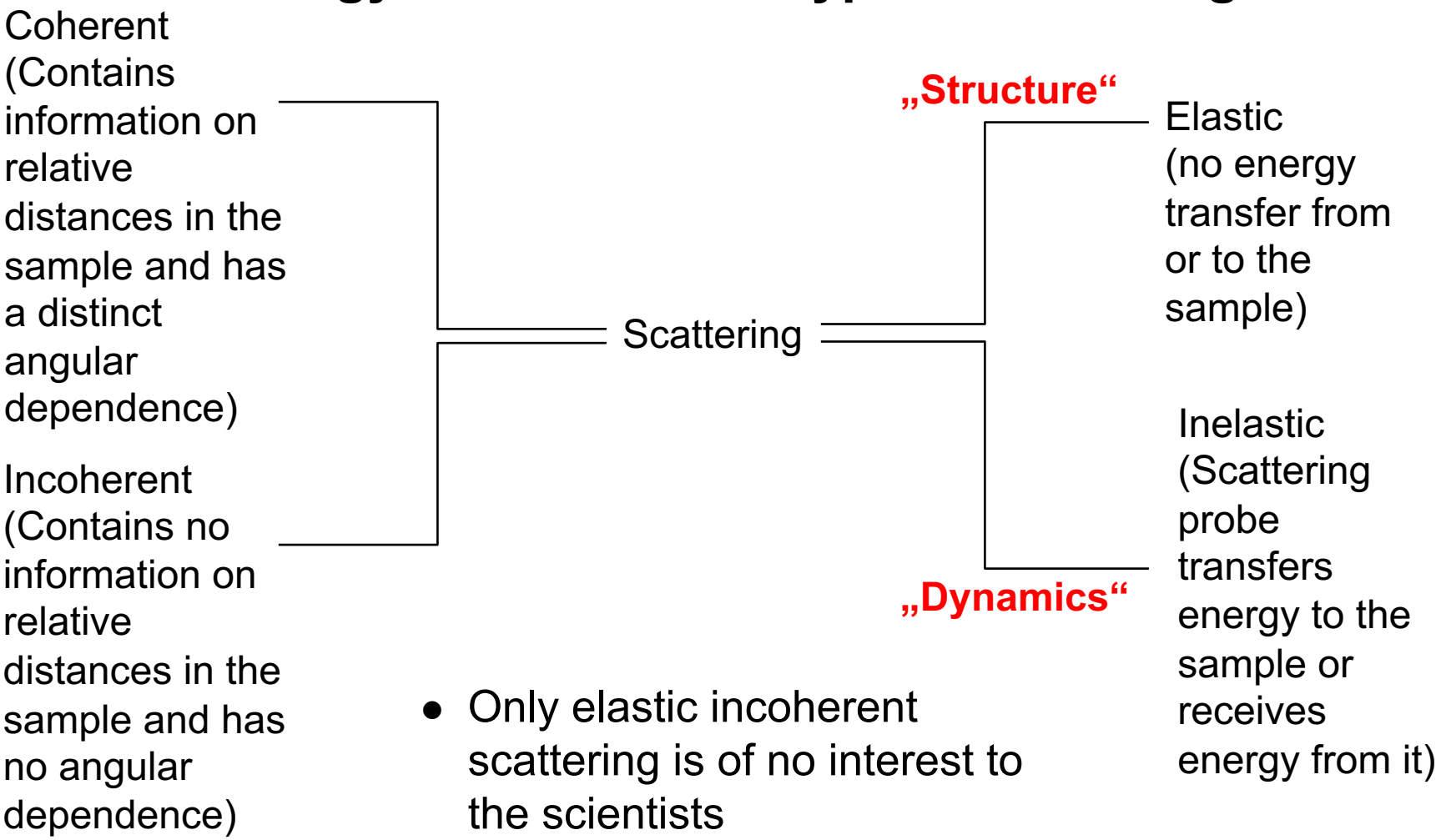

- Only elastic incoherent scattering is of no interest to the scientists

Neutron Spin Echo Spectroscopy

Only Inelastic scattering recorded, high energy resolution

Neutron Spin Echo Spectroscopy

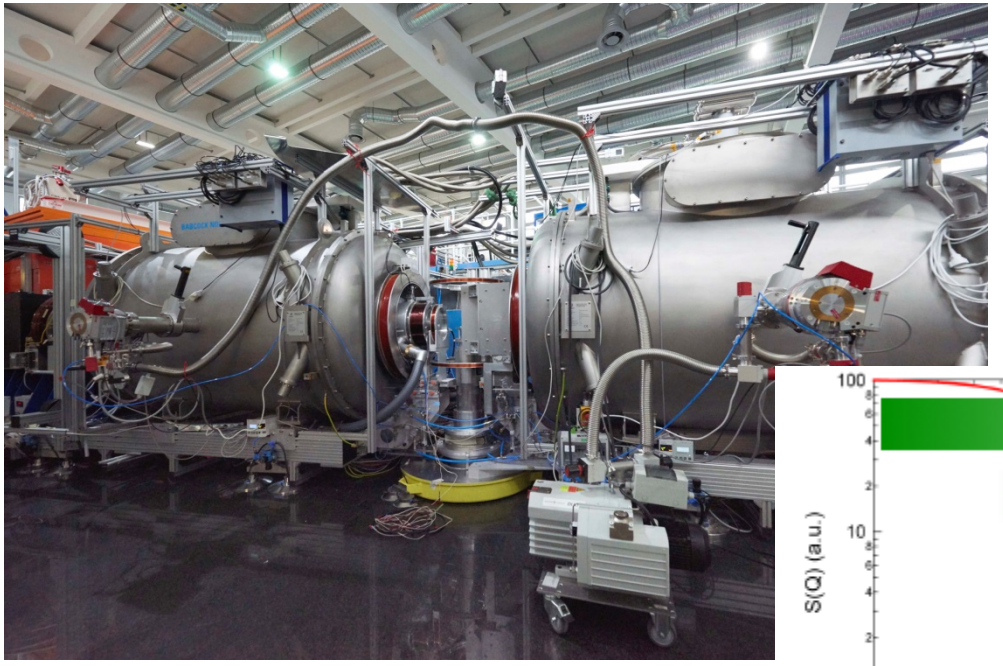

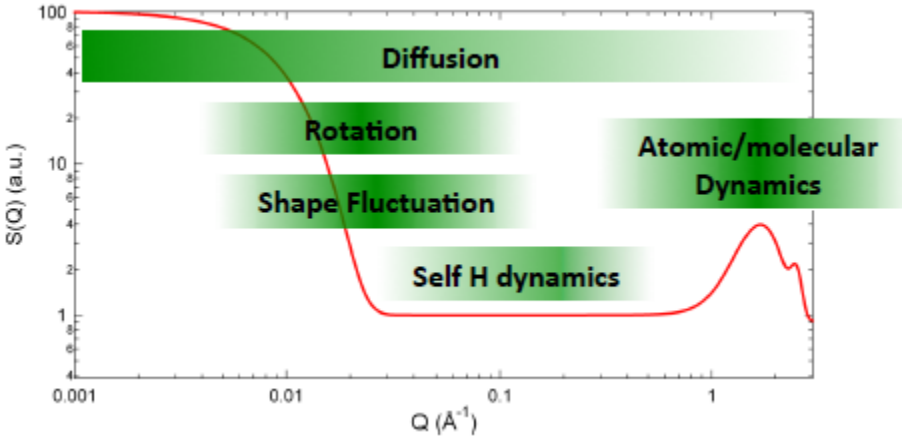

A. Farone: Methods and Applications of SANS, NR, and NSE NCNR, 2012

The Spin Echo Principle

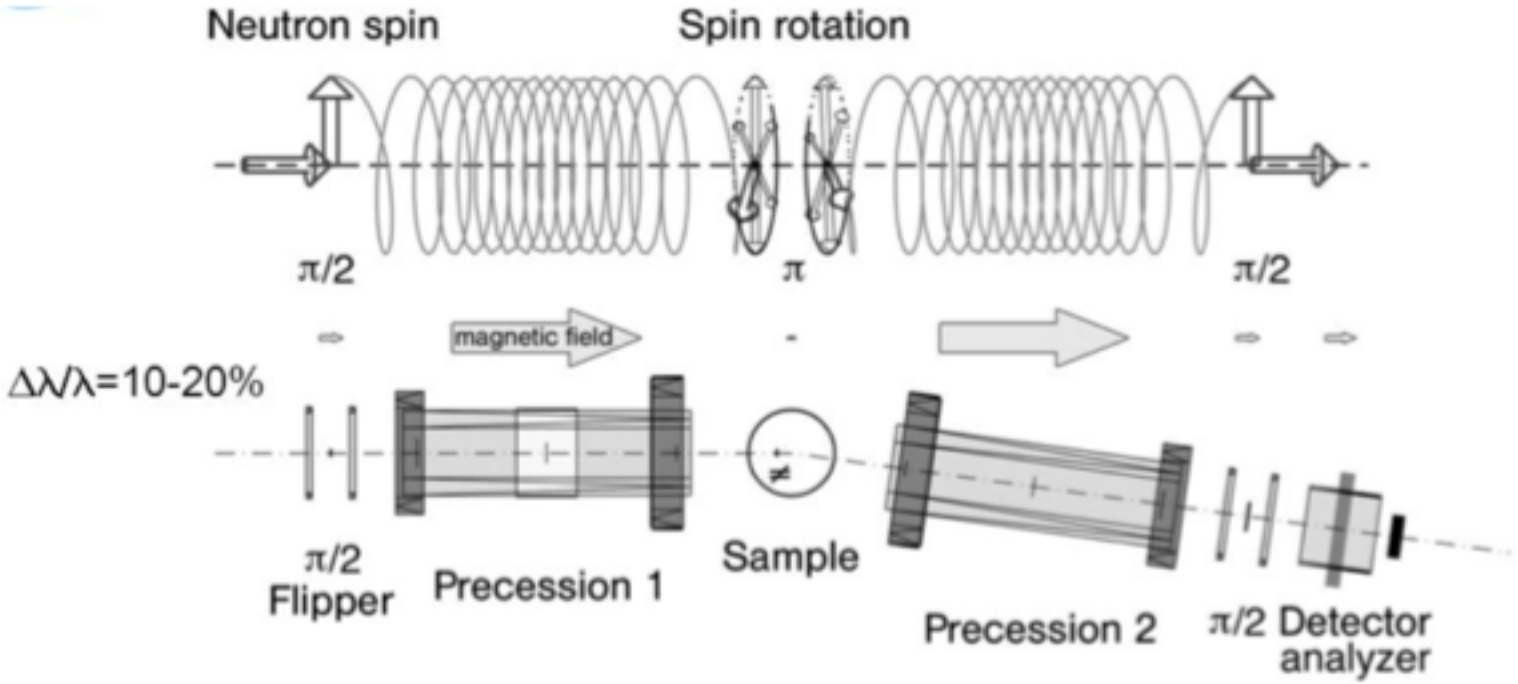

decoupling detectability of tiny velocity changes caused by the scattering process from the width of the incoming velocity distribution

the key is the neutron spin

Slide by A. Radulescu and Olaf Holderer

Phosphoglycerate kinase (PGK) as an enzyme

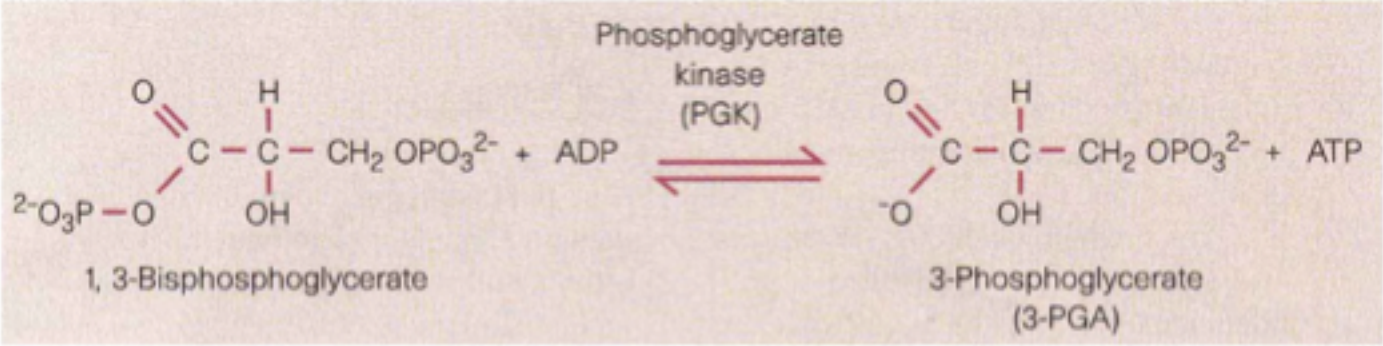

Phosphoglycerate kinase (PGK) catalyses a reversible phosphotransfer reaction that is normally involved in the production of ATP during glycolysis. Bernstein *et al.*[1] have crystallized an active form of PGK, using substrates — ADP and 3-PGA — that cannot be converted to products. They find that when both substrates are bound, the enzyme undergoes a conformational rearrangement that brings the two ligand-binding sites together.

from Colin et al. NATURE I VOL 385116 JANUARY 1997

Phosphoglycerate Kinase is sixth step in glycolysis to deliver energy from sugar by phosphate transfer

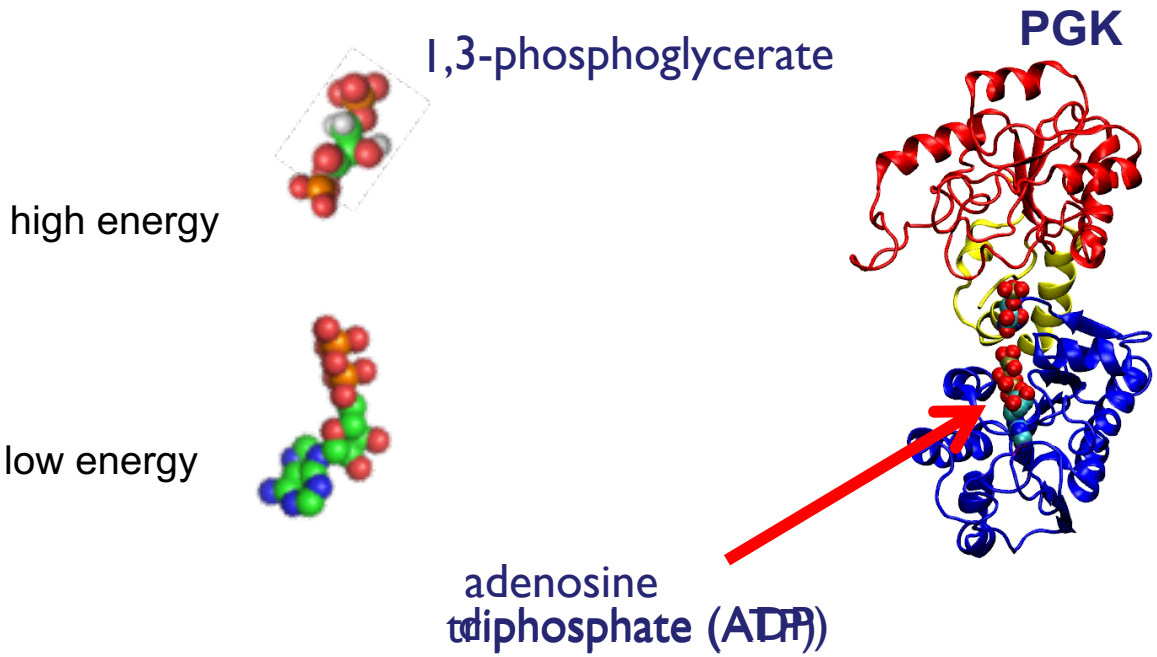

Structural change of Phosphoglycerate Kinase (PGK) due to substrate binding

yeast PGK
(relatet to glycolysis)

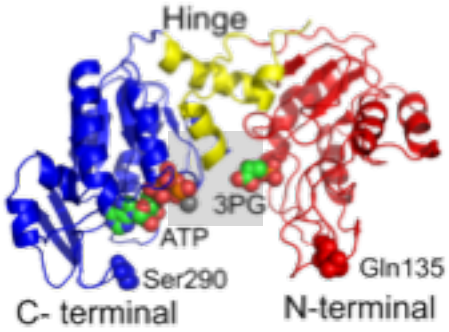

I(Q)*Q²

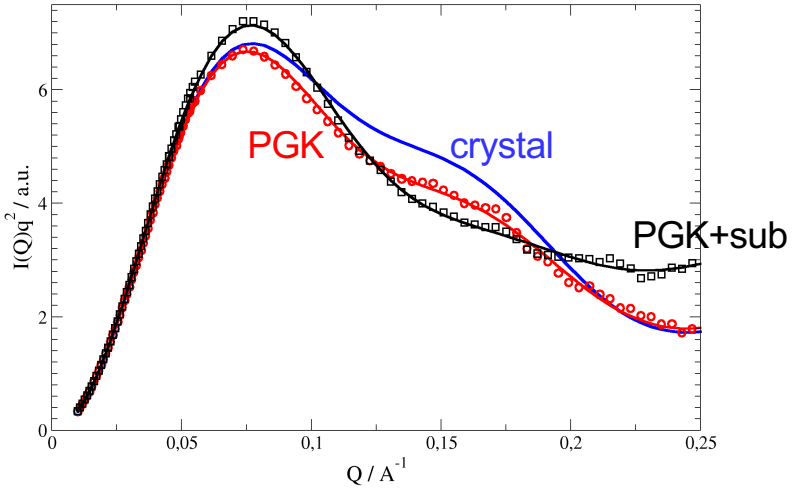

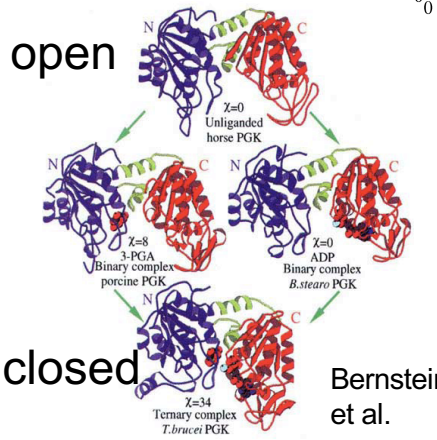

Bernstein
et al.

homologes
binding induces closing

Inoue et al. BiophysJ 99, 2309 (2010)

Elastic normal modes as templates for the structural change of PGK

yeast PGK
(relatet to glycolysis)

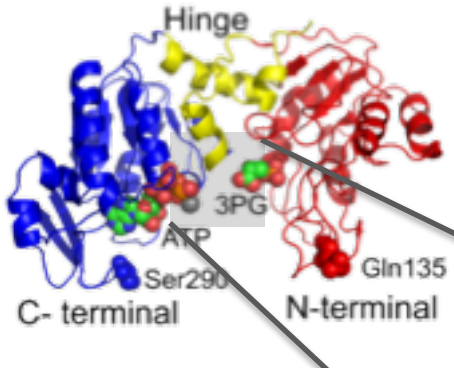

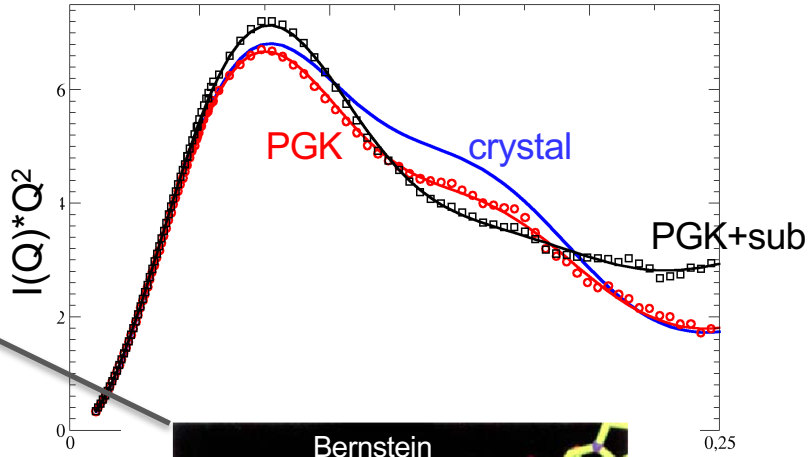

Arg38-Gly371

crystal	➔ 11.8 A
PGK	➔ 11.4 A
PGK+sub	➔ 8.2 A
active	➔ 3.5 A

activity not possible in **this** closed configuration with substrate bound

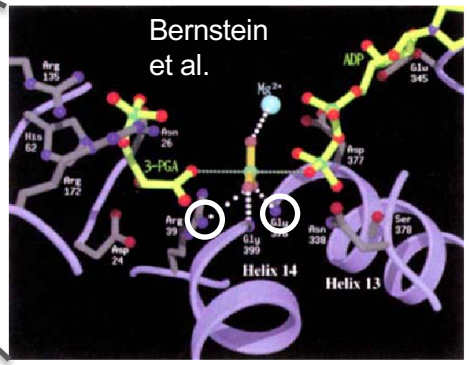

Inoue et al. BiophysJ 99, 2309 (2010)

Substrate binding reduces relaxation time and internal dynamics amplitude for PGK

internal dynamics

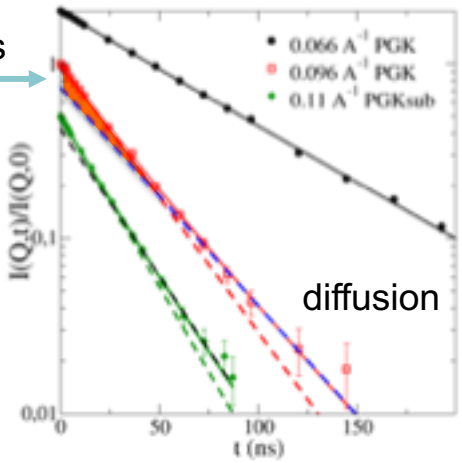

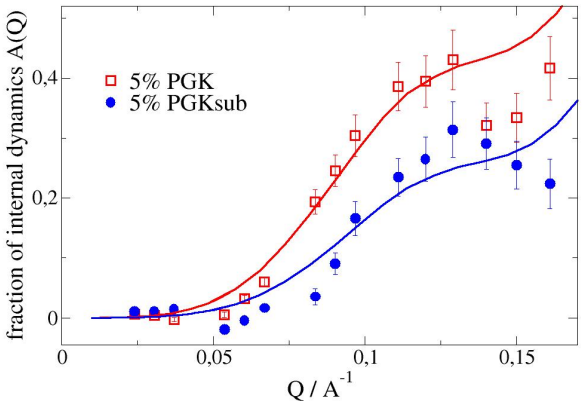

1/Γ=60(±10) ns PGK
1/Γ=45(±10) ns PGKsub

mean atomic displacement
10.5±2A for PGK
7.0±2A for PGKsub

mode 7 + mode 8 + mode 9 =

contribution of normal modes

Inoue et al. BiophysJ 99, 2309 (2010)

Domain dynamics is essential to reach catalytic configuration

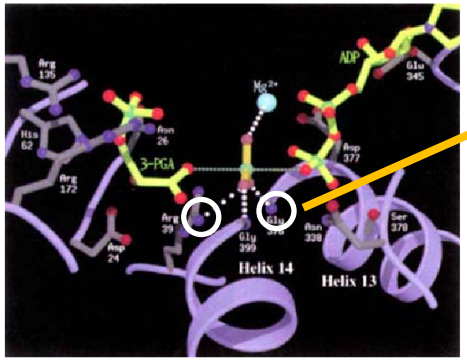

Bernstein et al. Nature 385, 275 (1997)

Figure 5 The active site of *T. brucei* PGK with the transition state modelled as a

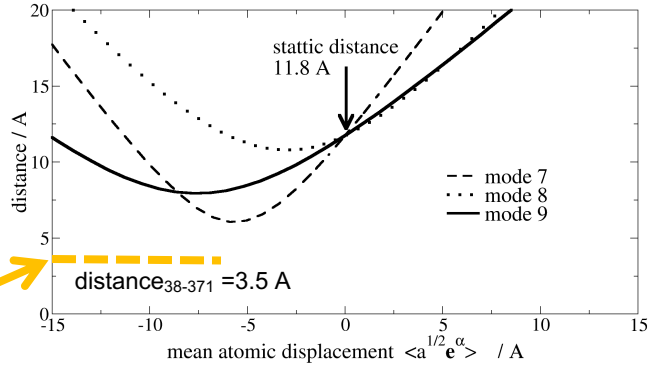

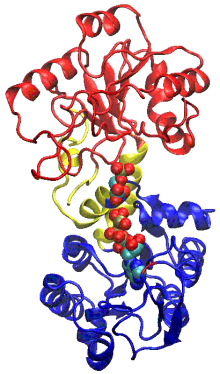

mode 7

Arg 38

Gly 371

Inoue et al. BiophysJ 99, 2309 (2010)

Spin Echo summary

Dynamics of (biological) macromolecules in solution (or in the melt) can be investigated without the need for (fluorescent) labels

Equilibrium dynamics (normal modes) are essential for the function of some enzymes

Summary

- Neutron protein crystallography is a complementary technique as compared to x-ray crystallography. Here one can determine:
  1. protonation states of amino acid side chains (important for the function of the protein)
  2. deuterium exchange as a measure of flexibility and accessibility (discrimination between **H** / **D**)
  3. solvent structure including hydrogen atoms

- Small angle neutron scattering: Here, the low resolution structure of sample in solution can be determined
- Contrast matching allows to ”hide” certain parts of the sample which then allows to measure the structure of the other part

Thanks to...

- Ralf Biehl
- Andreas Ostermann
- Marialucia Longo
- Livia Balacescu
- Florian Vögl
- Leo Rothmayer
- Olaf Holderer
- Aurel Radulescu

and thanks to Christian Betzel and Jeroen Mesters for organizing everything so well and for giving me the opportuinity to speak here

and you for your attention!

This project receives funding from the European Union's Horizon 2020 research and innovation programme under grant agreement No 654000

Bundesministerium für Bildung und Forschung

BMBF Verbundforschung funding is gratefully acknoledged: Förderkennzeichen: **05K16PA1**